Topocentric Orbit Determination: Algorithms for the Next Generation Surveys

Andrea Milani[1], Giovanni F. Gronchi[1], Davide Farnocchia[1],
Zoran Knežević[2] Robert Jedicke[3], Larry Denneau[3], Francesco Pierfederici[4]

[1] Department of Mathematics, University of Pisa, Largo Pontecorvo 5, 56127 Pisa, Italy

[2] Astronomical Observatory, Volgina 7, 11160 Belgrade 74, Serbia

[3] Pan-STARRS, Institute for Astronomy, University of Hawaii, 2680 Woodlawn Drive, Honolulu, Hawaii, 96822, USA

[4] LSST Corporation, 4703 E. Camp Lowell Drive, Suite 253, Tucson, Arizona, 85712, USA

Submitted to Icarus: 29 June 2007

Revised version: 25 September 2007

Manuscript pages: 52

Figures: 8; Tables: 10

Running head: Orbit Determination Algorithms

Send correspondence to:

Andrea Milani

Department of Mathematics

Largo Pontecorvo 5

56127 Pisa, Italy

Italy

e-mail: milani@dm.unipi.it

phone: +39-050-2213254 fax: +39-050-92213224;

ABSTRACT

Given a set of astrometric observations of the same object, the problem of orbit determination is to compute the orbit, assessing its uncertainty and reliability. For the next generation surveys, with much larger number density of observations, new algorithms, or at least substantial revisions of the classical ones, are needed. The problem has three main steps, preliminary orbit, least squares orbit, and quality control. The classical theory of preliminary orbit algorithms was incomplete, in that the consequences of the topocentric correction had not been fully studied. We show that it is possible to rigorously account for topocentric observations, possibly with an increase in the number of alternate preliminary orbits, without impairing the overall performance. We have developed modified least squares algorithms, including fitting with a reduced number of parameters; they can be used when the observed arcs have small curvature to improve the reliability of the orbit computing procedure. This requires suitable control logic to pipeline the different algorithms. We have tested the complete procedure on two simulations of the next generation all-sky surveys such as Pan-STARRS and LSST. False identification (where observations of different objects are incorrectly linked together) can be discarded with a quality control on the residuals and a procedure of normalization to remove duplications and contradictions in the output. The results confirm that large sets of discoveries can be obtained with good quality orbits and very high success rate, losing only 0.6 to 1.3% of objects and a false identification rate in the range 0.02 to 0.06%.

Key Words: Celestial Mechanics; Asteroids, Dynamics; Orbits

1 Introduction

The problem of preliminary orbit determination is old, with very effective solutions developed by [Laplace 1780] and [Gauss 1809]. However, the methods of observing Solar System bodies have changed radically since classical times and have been changing even faster recently due to advances in digital astrometry. The question is, what needs to be improved in the classical orbit determination algorithms to handle the expected rate of data from the next generation all-sky surveys? Alternatively, what can we now use in place of the classical algorithms?

The issue is not one of computational resources because these grow at the same rate as the capability of generating astrometric data. Reliability is the main problem when handling tens of millions of detections of Solar System objects. An algorithm failing once in $1,000$ usages may have been considered reliable a few years ago, but now we must demand better performance.

This is particularly important because of the strong correlation between difficulties in the orbit computation and the scientific value of the discovered object. Main Belt Asteroids (MBAs) are commonplace and their orbits are easily computed. Only a few in a $1,000$ of the objects (to a given limiting magnitude) are the more interesting Near Earth Objects (NEOs) while few in 100 are the equally interesting Trans Neptunian Objects (TNOs); in both cases the computation may be much more difficult for reasons explained later. Thus an algorithm computing orbits for 99% of the discoveries may be failing on a large fraction of the most interesting objects like NEOs and TNOs.

To understand the difference with the classical results one must take into account the change in the modern knowledge of the Solar System, as shown in the discussion above about NEOs and TNOs: the first TNO (Pluto) and the first Earth-Crossing asteroid (Apollo) were discovered only in 1930, after the publication of most of the preliminary orbit references, such as [Crawford et al. 1930]. Each of the classical results needs to be revisited to assess whether the assumptions are still appropriate. E.g., neglecting multiple preliminary orbits and dismissing the topocentric corrections is really wrong when searching for NEOs; neglecting the case in which the observed track in the sky has insignificant curvature is really wrong for TNOs. Another difference of context is the immensely superior computing power available to us: in the trade off between simpler and more reliable computations, we almost always select the latter, while the classical authors were forced to do the opposite.

In the following subsections we describe the content of this paper, emphasizing in particular the innovative features of our algorithms.

1.1 Problems and solutions: preliminary orbits

That Gauss' and Laplace's methods are, to some level of approximation, equivalent was known. We need to analyze precisely the approximations under which this is true, and to check whether they are still applicable under the current conditions. They are equivalent, up to the algebraic equation of degree 8, corresponding to a quadratic approximation in time, if the observations are geocentric. We show that with topocentric observations they are

not equivalent. As already pointed out by [Crawford et al. 1930, page 99] and [Marsden 1985], Gauss' method, at least in the version of [Merton 1925], can be used with topocentric observations employing the same formulae, Laplace's can not.

The difference between topocentric and geocentric observations is not negligible, apart from some special cases. The Laplace's method, as described in the literature, can account for topocentric observations, but only within an iterative procedure, the convergence of which is not guaranteed.

Laplace's method can be modified, following a suggestion by [Poincaré 1906], to account for topocentric observations already in the degree 8 equation. However, the qualitative theory of [Charlier 1910] allowing to compute the number of preliminary orbit solutions for Laplace's method does not apply to this modified version. It also does not apply to Gauss' method, and can not describe iterative methods.

When giving top priority to reliability, this is a problem: although it is always possible to improve the orbit with iterative methods, if the first approximation provides a wrong number of solutions it is possible to completely miss one convergent solution, which could be the actual one.

Using the basic formulae set up in Section 2, all the points above are discussed in Section 3.

Section 4 contains our solution of the problem. We have developed a new qualitative theory for the solutions of the equation of degree 8, for both Gauss' method and the modified Laplace-Poincaré, thus fully accounting for topocentric observations. We show that the number of solutions can be larger

than in Charlier's theory, e.g., there may be double solutions near opposition and triple solutions at low solar elongations. Some examples are given to show that the existence of additional solutions can affect the reliability of the orbit determination for real asteroids.

This progress tips the balance in favor of Gauss' method, handling topocentric observations in a natural way. An abstract qualitative theory is useful only if it is exploited by a software which can compute all solutions of the algebraic equations and keeps track of all of them; this was not the case so far [CITATION]. A tricky problem arises when, after the solution of the degree 8 equation, an iterative method is used to improve the preliminary orbit: the number of limit points of the iteration may be different from the number of starting solutions. We propose as an optimal compromise a two step procedure, in which the two versions, with and without iterative improvement, are used in sequence.

1.2 Problems and solutions: weakly determined orbits

The preliminary orbit methods fail when the quantities they use, essentially the curvature components, are so poorly determined that even their sign is uncertain. This happens when either the observed arc is too short or the object is very distant. In Section 5 we present how to detect when such poor conditions occur, and how to estimate the corresponding orbit uncertainty.

To deal with these low curvature cases we propose to use a *Virtual Asteroids (VA)* method. A VA is a complete orbit compatible with the available observations but by no means determined by them. A number of VA

are selected, either at random [Virtanen 2003] or by some geometric construction [Milani et al. 2004], among the orbits compatible with the observations. Many VA methods are found in the literature; for a recent review see [Milani 2005]. A very effective method for the problem at hand uses just one VA: it is derived from the theory of the *Admissible Region* [Milani et al. 2004].

Preliminary orbits are used as a first guess for the nonlinear optimization procedure (*Differential Corrections*) that computes the *nominal orbit* fulfilling the principle of *Least Squares* of the residuals. If the preliminary orbits are well defined, they are likely to belong to the convergence domain of some least squares orbit in the differential corrections; then it is sufficient to use all the preliminary orbits as first guesses. If the preliminary orbits are poorly defined they may be so far from the nominal solution that the differential corrections may not converge, even converge to the wrong solution.

Thus it is essential to increase the size of the convergence domain by using modified differential corrections methods. A number of these methods exist and most of them have one feature in common: the number of parameters determined is less than 6. There are 4-fit methods in which 2 variables are kept fixed and the others are corrected, e.g., [Milani et al. 2006]. There are 5-fit or *constrained least squares* solutions in which one parameter is fixed, although it does not need to be one of the orbital elements but may be defined in some intrinsic way [Milani et al. 2005a].

1.3 Numerical simulations and algorithms performances

To test the performance when our methods and software are confronted with the expected data rate and quality of the next generation surveys, we have used simulations of future surveys, with the source catalog as *ground truth*. This has been possible thanks to the collaboration with the Pan-STARRS [Jedicke et al. 2007] and LSST [Ivezić et al. 2007] projects.

We report in Section 6 on two tests, one based on small, focused simulations with only the most difficult orbits (NEOs and TNOs), and another representing the full data rate from a next generation survey with all classes of solar system objects (of course the numbers are dominated by MBAs).

The goal was to check that the reliability of our algorithms is good enough for the requirements of the next generation surveys. Moreover, we have checked which, among the new and/or improved algorithms discussed in this paper, are really necessary. The answer is that the performances can be very good also for the most difficult orbits, such as NEOs and TNOs, but for this all the innovative solutions we have proposed in this paper are essential, i.e., none of them is introduced just as a curiosity.

2 Equations from the Classical Theory

There are too many versions of preliminary orbit algorithms and there is no standard notation: it is not possible to simply copy the equations from some reference. We provide a compact summary of the basic formulae to be used in Sections 3-5, leading to the *dynamical equation* and the associated equation of degree 8 for both methods by Gauss and Laplace. We also summarize

Charlier's theory on the number of solutions for Laplace's method, to be compared to the new qualitative theory of Section 4.

2.1 Laplace's Method

The observation defines the unit vector $\hat{\boldsymbol{\rho}} = (\cos\delta\cos\alpha, \cos\delta\sin\alpha, \sin\delta)$ where (α, δ) are right ascension and declination. The heliocentric position of the observed body is

$$\mathbf{r} = \boldsymbol{\rho} + \mathbf{q} = \rho\hat{\boldsymbol{\rho}} + q\hat{\mathbf{q}}$$

where $\mathbf{q}$ is the observer's position. Let s be the arc length parameter for the path described by the relative position $\hat{\boldsymbol{\rho}}(t)$ and η the proper motion

$$\frac{ds}{dt} = \eta = \sqrt{\dot{\alpha}^2\cos^2\delta + \dot{\delta}^2}\ ;\ \frac{d}{ds} = \frac{1}{\eta}\frac{d}{dt}\ .$$

We use the moving orthonormal frame [Danby 1962, Sec. 7.1]

$$\hat{\boldsymbol{\rho}}\ ,\ \hat{\mathbf{v}} = \frac{d\hat{\boldsymbol{\rho}}}{ds}\ ,\ \hat{\mathbf{n}} = \hat{\boldsymbol{\rho}} \times \hat{\mathbf{v}} \tag{1}$$

and define the *geodesic curvature* κ by the equation

$$\frac{d\hat{\mathbf{v}}}{ds} = -\hat{\boldsymbol{\rho}} + \kappa\hat{\mathbf{n}}\ . \tag{2}$$

Then the relative acceleration is

$$\frac{d^2\boldsymbol{\rho}}{dt^2} = (\ddot{\rho} - \rho\eta^2)\hat{\boldsymbol{\rho}} + (\rho\dot{\eta} + 2\dot{\rho}\eta)\hat{\mathbf{v}} + (\rho\eta^2\kappa)\hat{\mathbf{n}} \tag{3}$$

and the differential equations of relative motions are

$$\frac{d^2\boldsymbol{\rho}}{dt^2} = \ddot{\mathbf{r}} - \ddot{\mathbf{q}} = \frac{\mu\mathbf{q}}{q^3} - \frac{\mu\mathbf{r}}{r^3} \tag{4}$$

with the following approximations: $\mathbf{q} = \mathbf{q}_\oplus$ coincides with the center of mass of the Earth, the only force operating on both the Earth and the object

at $\mathbf{r}$ is the gravitational attraction by the Sun, (no lunar and planetary perturbations, not even indirect perturbation by the Earth itself). From $(3)\cdot\hat{\mathbf{n}} = (4)\cdot\hat{\mathbf{n}}$

$$\frac{d^2\boldsymbol{\rho}}{dt^2}\cdot\hat{\mathbf{n}} = \rho\eta^2\kappa = \mu\, q\, \hat{\mathbf{q}}\cdot\hat{\mathbf{n}}\left(\frac{1}{q^3}-\frac{1}{r^3}\right)\ ,$$

which can be presented in the form

$$C\frac{\rho}{q} = 1-\frac{q^3}{r^3}\quad\text{where}\quad C=\frac{\eta^2\kappa q^3}{\mu\hat{\mathbf{q}}\cdot\hat{\mathbf{n}}} \tag{5}$$

referred to as the *dynamical equation* in the literature on preliminary orbits[1]. C is a non-dimensional quantity that can be 0 when $r = q$ or undetermined (of the form 0/0) in the case that the $O(\Delta t^2)$ approximation fails, *i.e.* the object is at an inflection point with tangent pointing to the Sun.

Given ρ, to complete the initial conditions $\dot{\rho}$ is solved from $(3)\cdot\hat{\mathbf{v}} = (4)\cdot\hat{\mathbf{v}}$

$$-\mu\frac{\boldsymbol{q}\cdot\hat{\mathbf{v}}}{r^3}+\mu\frac{\boldsymbol{q}\cdot\hat{\mathbf{v}}}{q^3} = \rho\dot{\eta}+2\dot{\rho}\eta\ . \tag{6}$$

The aberration can be accurately accounted for by using as epoch of the initial conditions the true time at the asteroid $t = t_{obs} - \rho/c$, where t_{obs} is the central time at which the observation $\hat{\boldsymbol{\rho}}$ has been taken and at which the derivatives have been interpolated [Crawford et al. 1930, page 99].

Eq. (5) is the basic formula for Laplace's method using the solution in terms of either ρ or r which are not independent quantities. From the triangle formed by the vectors $\mathbf{q}, \boldsymbol{\rho}, \mathbf{r}$ we have the *geometric equation*

$$r^2 = \rho^2 + 2\rho q\cos\varepsilon + q^2 \tag{7}$$

[1]It is actually the component of the equations of motion along the normal to the path.

where $\cos\varepsilon = \hat{\mathbf{q}} \cdot \hat{\boldsymbol{\rho}}$ is fixed by the observation direction ($\varepsilon = 180°-$ solar elongation). By substituting ρ from eq. (7) in (5), squaring and multiplying by $C^2\, r^6$ ($C \neq 0$, otherwise $r = q$, the *zero circle*) we obtain

$$P(r) = C^2 r^8 - q^2 r^6 (1 + 2C\cos\varepsilon + C^2) + 2q^5 r^3 (1 + C\cos\varepsilon) - q^8 = 0\ . \quad (8)$$

The trivial root $r = q$ is due to a coordinate singularity. There can be other *spurious solutions* of the equation (8) corresponding to $\rho < 0$ in eq. (5).

2.2 Charlier's Theory

The qualitative theory of [Charlier 1910] on the number of solutions is obtained by analyzing equations (5)-(8). The sign of the coefficients of eq. (8) is known: $-(1+2C\cos\varepsilon+C^2) < 0$ and $(1+C\cos\varepsilon) > 0$ (see [Plummer 1918]). Thus there are 3 changes of sign in the sequence of coefficients and ≤ 3 positive real roots. By extracting the factor $(r - q)$

$$P(r) = (r-q)\ P_1(r) \quad ; \quad P_1(0) = q^7 \quad ; \quad P_1(q) = q^7\ C\ (C - 3\cos\varepsilon)\ .$$

The number of solutions of the polynomial equation changes where $P_1(q)$ changes sign, at $C = 0 \Leftrightarrow r = q$ and at $C - 3\cos\varepsilon = 0$. The latter condition defines the *limiting curve*; in heliocentric polar coordinates (r, ϕ), by using $\rho^2 = r^2 + q^2 - 2\, r\, q\, \cos\phi$,

$$4 - 3\frac{r}{q}\cos\phi = \frac{q^3}{r^3}\ . \quad (9)$$

Figure 1

Following [Charlier 1910, Charlier 1911], the number of solutions can be understood by a plot of the level curves of the function $C(r, \rho)$ defined by

the dynamical equation, in a plane with the Sun at $(0, 0)$, the Earth at $(q, 0)$ and the position in each half-plane defined by the bipolar coordinates (r, ρ). The limiting curve and the zero circle can be used to deduce the number of solutions occurring at the discovery of an object located at any point of the plane[2]. There is only one solution on the right of the unlimited branches of the limiting curve, around opposition. There are two solutions for every point between the unlimited branches and the zero circle. Inside the zero circle and outside the loop of the limiting curve there is only one solution. Inside that loop there are always two solutions.

Charlier's theory assumes there is always at least one preliminary orbit solution. This results from two implicit assumptions: the value of C is measured exactly, or at least to good accuracy, from the observations, and the observed object exists (not being the result of a false identification). Both assumptions may fail as discussed in Section 5 and 6.2, respectively.

2.3 Gauss' Method

Gauss' method uses 3 observations corresponding to heliocentric positions

$$\mathbf{r}_i = \boldsymbol{\rho}_i + \mathbf{q}_i \quad i = 1, 2, 3 \tag{10}$$

at times $t_1 < t_2 < t_3$ with $t_i - t_j = \mathcal{O}(\Delta t) \ll$ period and the condition of coplanarity:

$$\lambda_1 \mathbf{r}_1 - \mathbf{r}_2 + \lambda_3 \mathbf{r}_3 = 0 \ . \tag{11}$$

[2]This plane does not correspond to a physical plane in that it also describes the points outside the ecliptic plane.

From (11)$\times \mathbf{r}_i \cdot \hat{\mathbf{c}}$, where $\mathbf{c} = \mathbf{r}_i \times \dot{\mathbf{r}}_i$, the coefficients λ_1, λ_3 are obtained as *triangle ratios*

$$\lambda_1 = \frac{\mathbf{r}_2 \times \mathbf{r}_3 \cdot \hat{\mathbf{c}}}{\mathbf{r}_1 \times \mathbf{r}_3 \cdot \hat{\mathbf{c}}} \;\; ; \;\; \lambda_3 = \frac{\mathbf{r}_1 \times \mathbf{r}_2 \cdot \hat{\mathbf{c}}}{\mathbf{r}_1 \times \mathbf{r}_3 \cdot \hat{\mathbf{c}}} \; .$$

From (10) and $\hat{\boldsymbol{\rho}}_1 \times \hat{\boldsymbol{\rho}}_3 \cdot$(11):

$$\rho_2[\hat{\boldsymbol{\rho}}_1 \times \hat{\boldsymbol{\rho}}_3 \cdot \hat{\boldsymbol{\rho}}_2] = \hat{\boldsymbol{\rho}}_1 \times \hat{\boldsymbol{\rho}}_3 \cdot [\lambda_1 \mathbf{q}_1 - \mathbf{q}_2 + \lambda_3 \mathbf{q}_3]. \tag{12}$$

Next, the differences $\mathbf{r}_i - \mathbf{r}_2$ are expanded in powers of $t_{ij} = t_i - t_j = \mathcal{O}(\Delta t)$. e.g. by using the f, g series formalism $\mathbf{r}_i = f_i \mathbf{r}_2 + g_i \dot{\mathbf{r}}_2$

$$f_i = 1 - \frac{\mu}{2} \frac{t_{i2}^2}{r_2^3} + \mathcal{O}(\Delta t^3) \quad , \quad g_i = t_{i2} \left(1 - \frac{\mu}{6} \frac{t_{i2}^2}{r_2^3} \right) + \mathcal{O}(\Delta t^4) \; . \tag{13}$$

Then $\mathbf{r}_i \times \mathbf{r}_2 = -g_i \mathbf{c}$, $\mathbf{r}_1 \times \mathbf{r}_3 = (f_1 g_3 - f_3 g_1)\mathbf{c}$ and

$$\lambda_1 = \frac{g_3}{f_1 g_3 - f_3 g_1} > 0 \; ; \; \lambda_3 = \frac{-g_1}{f_1 g_3 - f_3 g_1} > 0 \tag{14}$$

$$f_1 g_3 - f_3 g_1 = t_{31} \left(1 - \frac{\mu}{6} \frac{t_{31}^2}{r_2^3} \right) + \mathcal{O}(\Delta t^4) \; . \tag{15}$$

Using (13) and (15) in (14)

$$\lambda_1 = \frac{t_{32}}{t_{31}} \left[1 + \frac{\mu}{6 r_2^3} (t_{31}^2 - t_{32}^2) \right] + \mathcal{O}(\Delta t^3) \; . \tag{16}$$

$$\lambda_3 = \frac{t_{21}}{t_{31}} \left[1 + \frac{\mu}{6 r_2^3} (t_{31}^2 - t_{21}^2) \right] + \mathcal{O}(\Delta t^3) \; . \tag{17}$$

Let $P = \hat{\boldsymbol{\rho}}_1 \times \hat{\boldsymbol{\rho}}_2 \cdot \hat{\boldsymbol{\rho}}_3$ be 3$\times$volume of the pyramid with vertices $\mathbf{q}, \mathbf{r}_1, \mathbf{r}_2, \mathbf{r}_3$; by substituting it and (16), (17) in (12), using $t_{31}^2 - t_{32}^2 = t_{21}(t_{31} + t_{32})$ and $t_{31}^2 - t_{21}^2 = t_{32}(t_{31} + t_{21})$

$$-P \rho_2 t_{31} = \hat{\boldsymbol{\rho}}_1 \times \hat{\boldsymbol{\rho}}_3 \cdot (t_{32} \mathbf{q}_1 - t_{31} \mathbf{q}_2 + t_{21} \mathbf{q}_3) + \tag{18}$$

$$+ \hat{\boldsymbol{\rho}}_1 \times \hat{\boldsymbol{\rho}}_3 \cdot \left[\frac{\mu}{6 r_2^3} [t_{32} t_{21} (t_{31} + t_{32}) \mathbf{q}_1 + t_{32} t_{21} (t_{31} + t_{21}) \mathbf{q}_3] \right] + \mathcal{O}(\Delta t^4) \; .$$

If the terms $\mathcal{O}(\Delta t^4)$ are neglected, the coefficient of the $1/r_2^3$ term in (18) is

$$B(\mathbf{q}_1, \mathbf{q}_3) = \frac{\mu}{6} t_{32} t_{21} \hat{\boldsymbol{\rho}}_1 \times \hat{\boldsymbol{\rho}}_3 \cdot [(t_{31} + t_{32})\mathbf{q}_1 + (t_{31} + t_{21})\mathbf{q}_3]. \tag{19}$$

Then multiply (18) by $q_2^3/B(\mathbf{q}_1, \mathbf{q}_3)$ to obtain

$$-\frac{P\ \rho_2\ t_{31}}{B(\mathbf{q}_1, \mathbf{q}_3)}\ q_2^3 = \frac{q_2^3}{r_2^3} + \frac{A(\mathbf{q}_1, \mathbf{q}_2, \mathbf{q}_3)}{B(\mathbf{q}_1, \mathbf{q}_3)}$$

where

$$A(\mathbf{q}_1, \mathbf{q}_2, \mathbf{q}_3) = q_2^3\ \hat{\boldsymbol{\rho}}_1 \times \hat{\boldsymbol{\rho}}_3 \cdot [t_{32}\mathbf{q}_1 - t_{31}\mathbf{q}_2 + t_{21}\mathbf{q}_3]. \tag{20}$$

Let

$$C_0 = \frac{P\ t_{31}\ q_2^4}{B(\mathbf{q}_1, \mathbf{q}_3)} \quad , \quad h_0 = -\frac{A(\mathbf{q}_1, \mathbf{q}_2, \mathbf{q}_3)}{B(\mathbf{q}_1, \mathbf{q}_3)}$$

and then

$$C_0 \frac{\rho_2}{q_2} = h_0 - \frac{q_2^3}{r_2^3} \tag{21}$$

is the *dynamical equation* of Gauss' method, similar (but not identical) to eq. (5) of Laplace's method. Using (7) at time t_2 (with q_2, ρ_2, r_2 and ε_2):

$$P_0(r) = C_0^2 r_2^8 - q_2^2 r_2^6 (h_0^2 + 2C_0 h_0 \cos\varepsilon_2 + C_0^2) + 2q_2^5 r_2^3 (h_0 + C_0 \cos\varepsilon_2) - q_2^8 = 0 \tag{22}$$

where the sign of the coefficients is as for (8), apart from $h_0 + C_0 \cos\varepsilon_2$ whose sign may change depending upon h_0. Note that $P_0(q) \neq 0$, no root can be found analytically. The number of positive roots is still ≤ 3 but a qualitative theory such as the one of Section 2.2 is not available in the literature.

After the possible values for r_2 have been found the corresponding ρ_2 values are obtained from eq. (21) and the velocity $\dot{\mathbf{r}}_2$ can be computed, e.g. from the classical formulae by Gibbs [Herrick 1971, Chap. 8].

3 Topocentric Gauss-Laplace Methods

The critical difference between the methods of Gauss and Laplace is the following. Gauss uses a truncation (to order $\mathcal{O}(\Delta t^2)$) in the motion $\mathbf{r}(t)$ of the asteroid but the positions of the observer (be it coincident with the center of the Earth or not) are used in their exact values. Laplace uses a truncation to the same order of the relative motion $\boldsymbol{\rho}(t)$ (see eq.(30) in Section 5.1), thus implicitly approximating the motion of the observer. In this section we examine the consequences of the difference between the techniques.

3.1 Gauss-Laplace equivalence

To directly compare the two methods let us introduce in Gauss' method the same approximation to order $\mathcal{O}(\Delta t^2)$ in the motion of the Earth which is still assumed to coincide with the observer. The f, g series for Earth are

$$\mathbf{q}_i = \left(1 - \frac{\mu}{2}\frac{t_{i2}^2}{q_2^3}\right)\mathbf{q}_2 + t_{i2}\dot{\mathbf{q}}_2 + \frac{\mu}{6}\frac{t_{i2}^3}{q_2^3}\left[\frac{3(\mathbf{q}_2\cdot\dot{\mathbf{q}}_2)\mathbf{q}_2}{q_2^2} - \dot{\mathbf{q}}_2\right] + \mathcal{O}(\Delta t^4) \qquad (23)$$

By using (23) in (19) we find that

$$B(\mathbf{q}_1,\mathbf{q}_3) = \frac{\mu}{6}t_{32}t_{21}\hat{\boldsymbol{\rho}}_1\times\hat{\boldsymbol{\rho}}_3\cdot[3t_{31}\mathbf{q}_2 + t_{31}(t_{32}-t_{21})\dot{\mathbf{q}}_2 + \mathcal{O}(\Delta t^3)].$$

If $t_{32} - t_{21} = t_3 + t_1 - 2t_2 = 0$, that is, the interpolation for d^2/dt^2 is done at the central value t_2, then

$$B(\mathbf{q}_1,\mathbf{q}_3) = \frac{\mu}{2}t_{21}t_{32}t_{31}\hat{\boldsymbol{\rho}}_1\times\hat{\boldsymbol{\rho}}_3\cdot\mathbf{q}_2\,(1+\mathcal{O}(\Delta t^2))\ ;$$

else, if $t_2 \neq (t_1+t_3)/2$ the last factor is just $(1+\mathcal{O}(\Delta t))$. Using (23) in (20)

$$A(\mathbf{q}_1,\mathbf{q}_2,\mathbf{q}_3) = -\frac{\mu}{2}t_{21}t_{32}t_{31}\ \hat{\boldsymbol{\rho}}_1\times\hat{\boldsymbol{\rho}}_3\cdot\left\{\mathbf{q}_2 + \frac{1}{3}\,(t_{21}-t_{32})\left[\frac{3(\mathbf{q}_2\cdot\dot{\mathbf{q}}_2)\mathbf{q}_2}{q_2^2} - \dot{\mathbf{q}}_2\right]\right\} + \mathcal{O}(\Delta t^5).$$

If, as above, $t_{32} - t_{21} = t_3 + t_1 - 2t_2 = 0$ then

$$A(\mathbf{q}_1, \mathbf{q}_2, \mathbf{q}_3) = -\frac{\mu}{2} t_{21} t_{32} t_{31} \hat{\boldsymbol{\rho}}_1 \times \hat{\boldsymbol{\rho}}_3 \cdot \mathbf{q}_2 \, (1 + \mathcal{O}(\Delta t^2))$$

and we can conclude

$$h_0 = -\frac{A}{B} = 1 + \mathcal{O}(\Delta t^2) \; ;$$

else, if $t_2 \neq (t_1 + t_3)/2$ the last factor is just $(1 + \mathcal{O}(\Delta t))$. For P we need

$$\frac{d^2 \hat{\boldsymbol{\rho}}}{dt^2} = \frac{d \dot{\hat{\boldsymbol{\rho}}}}{dt} = \frac{d}{dt}(\eta \hat{\mathbf{v}}) = -\eta^2 \hat{\boldsymbol{\rho}} + \dot{\eta} \hat{\mathbf{v}} + \kappa \eta^2 \hat{\mathbf{n}} \tag{24}$$

to make a Taylor expansion of $\hat{\boldsymbol{\rho}}_i$ in t_2

$$\hat{\boldsymbol{\rho}}_i = \hat{\boldsymbol{\rho}}_2 + t_{i2} \eta \hat{\mathbf{v}}_2 + \frac{t_{i2}^2}{2}(-\eta^2 \hat{\boldsymbol{\rho}}_2 + \dot{\eta} \hat{\mathbf{v}}_2 + \kappa \eta^2 \hat{\mathbf{n}}_2) + \mathcal{O}(\Delta t^3).$$

This implies that

$$\hat{\boldsymbol{\rho}}_1 \times \hat{\boldsymbol{\rho}}_3 \cdot \hat{\boldsymbol{\rho}}_2 = \frac{1}{2} \left[t_{12} \eta \hat{\mathbf{v}}_2 \times t_{32}^2 \kappa \, \eta^2 \hat{\mathbf{n}}_2 - t_{32} \eta \, \hat{\mathbf{v}}_2 \times t_{12}^2 \kappa \, \eta^2 \, \hat{\mathbf{n}}_2 \right] \cdot \hat{\boldsymbol{\rho}}_2 + \mathcal{O}(\Delta t^5)$$

and the $\mathcal{O}(\Delta t^4)$ term vanishes. Thus

$$P = -\frac{\kappa \eta^3}{2}(t_{12} t_{32}^2 - t_{32} t_{12}^2) \, (1 + \mathcal{O}(\Delta t^2)) = \frac{\kappa \eta^3}{2} t_{21} t_{32} t_{31} \, (1 + \mathcal{O}(\Delta t^2))$$

$$C_0 = \frac{P t_{31} q_2^4}{B} = \frac{\kappa \eta^3 t_{31} q_2^4 + \mathcal{O}(\Delta t^3)}{\mu \hat{\boldsymbol{\rho}}_1 \times \hat{\boldsymbol{\rho}}_3 \cdot \mathbf{q}_2 \, (1 + \mathcal{O}(\Delta t))}. \tag{25}$$

In the denominator, $\hat{\boldsymbol{\rho}}_1 \times \hat{\boldsymbol{\rho}}_3$ computed to order Δt^2 is

$$\hat{\boldsymbol{\rho}}_1 \times \hat{\boldsymbol{\rho}}_3 = t_{31} \, \eta \, \hat{\mathbf{n}}_2 + \frac{t_{32}^2 - t_{12}^2}{2} \, (\dot{\eta} \, \hat{\mathbf{n}}_2 - \kappa \, \eta^2 \, \hat{\mathbf{v}}_2) + \mathcal{O}(\Delta t^3). \tag{26}$$

If $t_{32} - t_{21} = t_3 + t_1 - 2t_2 = 0$ then

$$C_0 = \frac{\kappa \, \eta^3 \, t_{31} q_2^4 + \mathcal{O}(\Delta t^3)}{\mu \, t_{31} \, \eta \, q_2 \hat{\mathbf{q}}_2 \cdot \hat{\mathbf{n}}_2 + \mathcal{O}(\Delta t^3)} = \frac{\kappa \, \eta^2 \, q_2^3}{\mu \, \hat{\mathbf{q}}_2 \cdot \hat{\mathbf{n}}_2} \, (1 + (\mathcal{O} \Delta t^2)) \; ,$$

otherwise the last factor is $(1 + \mathcal{O}(\Delta t))$.

Thus, neglecting the difference between topocentric and geocentric observations, the coefficients of the two dynamical equations (5) and (21) are the same to zero order in Δt, also to order 1 if the time t_2 is the average time.

3.2 Topocentric Laplace's Method

Now let us remove the approximation that the observer sits at the center of the Earth and introduce *topocentric observations* into Laplace's method. The center of mass of the Earth is at $\mathbf{q}_\oplus$ but the observer is at $\mathbf{q} = \mathbf{q}_\oplus + \mathbf{P}$. Let us derive the dynamical equation by also taking into account the acceleration contained in the geocentric position of the observer $\mathbf{P}(t)$ such that

$$\frac{d^2\boldsymbol{\rho}}{dt^2} = -\frac{\mu \mathbf{r}}{r^3} + \frac{\mu \mathbf{q}_\oplus}{q_\oplus^3} - \ddot{\mathbf{P}}.$$

Multiplying by $\cdot\hat{\mathbf{n}}$ and using eq. (3)

$$\frac{d^2\boldsymbol{\rho}}{dt^2} \cdot \hat{\mathbf{n}} = \rho\eta^2\kappa = \mu \left[q_\oplus \frac{\hat{\mathbf{q}}_\oplus \cdot \hat{\mathbf{n}}}{q_\oplus^3} - q_\oplus \frac{\hat{\mathbf{q}}_\oplus \cdot \hat{\mathbf{n}}}{r^3} - P \frac{\hat{\mathbf{P}} \cdot \hat{\mathbf{n}}}{r^3} \right] - \ddot{\mathbf{P}} \cdot \hat{\mathbf{n}}$$

The term $P\,\hat{\mathbf{P}} \cdot \hat{\mathbf{n}}/r^3$ can be neglected. This approximation is legitimate because $P/q_\oplus \leq 4.3 \times 10^{-5}$ and the neglected term is smaller than the planetary perturbations. Thus

$$C\frac{\rho}{q_\oplus} = (1 - \Lambda_n) - \frac{q_\oplus^3}{r^3} \tag{27}$$

where

$$C = \frac{\eta^2 \kappa q_\oplus^3}{\mu \hat{\mathbf{q}}_\oplus \cdot \hat{\mathbf{n}}} \quad , \quad \Lambda_n = \frac{q_\oplus^2 \ddot{\mathbf{P}} \cdot \hat{\mathbf{n}}}{\mu \hat{\mathbf{q}}_\oplus \cdot \hat{\mathbf{n}}} = \frac{\ddot{\mathbf{P}} \cdot \hat{\mathbf{n}}}{(\mu/q_\oplus^2)\, \hat{\mathbf{q}}_\oplus \cdot \hat{\mathbf{n}}}. \tag{28}$$

Note that Λ_n is singular only where C is also singular. The analog of eq. (6), again neglecting $\mathcal{O}(p/q_\oplus)$, is

$$\rho\dot{\eta} + 2\dot{\rho}\eta = \frac{\mu\ \hat{\mathbf{q}}_\oplus \cdot \hat{\mathbf{v}}}{q_\oplus^2} \left(1 - \Lambda_v - \frac{q_\oplus^3}{r^3} \right) \quad , \quad \Lambda_v = \frac{q_\oplus^2\ \ddot{\mathbf{P}} \cdot \hat{\mathbf{v}}}{\mu\ \hat{\mathbf{q}}_\oplus \cdot \hat{\mathbf{v}}}\ . \tag{29}$$

The important fact is that Λ_n and Λ_v are by no means small. The centripetal acceleration of the observer (towards the rotation axis of the Earth) has size $|\ddot{\mathbf{P}}| = \Omega_\oplus^2\, R_\oplus \cos\theta$ where $\Omega_\oplus$ is the angular velocity of the Earth's rotation,

$R_\oplus$ the radius of the Earth and θ the latitude; the maximum of $\simeq 3.4\ cm\, s^{-2}$ occurs at the equator. The quantity $\mu/q_\oplus^2$ in the denominator of Λ_n is the size of the heliocentric acceleration of the Earth, $\simeq 0.6\ cm\, s^{-2}$. Thus $|\Lambda_n|$ can be > 1, and the coefficient $1 - \Lambda_n$ very different from 1; it may even be negative. Without taking into account the geocentric acceleration of the observer, the classical method of Laplace is not a good approximation in the general case. When the observations of different nights are taken from the same station at the same sidereal time the observer's acceleration cancels out, and the classical Laplace method is a good approximation.

The common procedure for Laplace's method is to apply a negative topocentric correction to go back to the geocentric observation case. However, in doing this some value of ρ is assumed as a first approximation, e.g., $\rho = 1\ AU$ [Leuschner, 1913, Page 15]. If this value is approximately correct, by iterating the cycle (topocentric correction - Laplace's determination of ρ) convergence is achieved. If the starting value is really wrong, e.g., if the object is undergoing a close approach to the Earth, the procedure may well diverge. These reliability problems discourage the use of the classical form of Laplace's method when processing a large dataset, containing discoveries of different orbital classes and therefore spanning a wide range of distances.

3.3 Gauss-Laplace equivalence, topocentric

When taking into account the displacement $\mathbf{P}$ the Taylor expansion of $\mathbf{q}_i(t)$ of eq. (23) is not applicable. We need to use

$$\mathbf{q}_i = \mathbf{q}_2 + t_{i2}\dot{\mathbf{q}}_2 + \frac{t_{i2}^2}{2}\ddot{\mathbf{q}}_2 + \mathcal{O}(\Delta t^3)$$

where $\mathbf{q}_2(t)$ and its derivatives contain also $\mathbf{P}(t)$. By using eq. (26) and assuming $t_{21} = t_{32}$, eq. (19) and (20) become

$$B(\mathbf{q}_1, \mathbf{q}_3) = \frac{\mu\ \eta}{2}\ t_{21} t_{32} t_{31}^2\ \hat{\mathbf{n}}_2 \cdot \mathbf{q}_2 + \mathcal{O}(\Delta t^6)$$

$$A(\mathbf{q}_1, \mathbf{q}_2, \mathbf{q}_3) = \frac{q_2^3\ \eta}{2}\ t_{21} t_{32} t_{31}^2\ \hat{\mathbf{n}}_2 \cdot \ddot{\mathbf{q}}_2 + \mathcal{O}(\Delta t^6)\ .$$

Note that $\dot{\mathbf{q}}_2$ does not appear in A at this approximation level. Thus

$$h_0 = -\frac{A}{B} = -\frac{q_2^3\ \hat{\mathbf{n}}_2 \cdot \ddot{\mathbf{q}}_2 + \mathcal{O}(\Delta t^2)}{\mu\ \hat{\mathbf{n}}_2 \cdot \mathbf{q}_2 + \mathcal{O}(\Delta t^2)}$$

and once again neglecting $P/q_\oplus$ terms

$$h_0 = -\frac{q_2^3\ \hat{\mathbf{n}}_2 \cdot \ddot{\mathbf{q}}_{\oplus 2}}{\mu\ \hat{\mathbf{n}}_2 \cdot \mathbf{q}_2} - \frac{q_2^3\ \hat{\mathbf{n}}_2 \cdot \ddot{\mathbf{P}}_2}{\mu\ \hat{\mathbf{n}}_2 \cdot \mathbf{q}_2} + O(\Delta t^2) =$$

$$= \frac{q_2^3}{q_{\oplus 2}^3} - \frac{q_2^3\ \hat{\mathbf{n}}_2 \cdot \ddot{\mathbf{P}}_2}{\mu\ \hat{\mathbf{n}}_2 \cdot \mathbf{q}_2} + \mathcal{O}(\Delta t^2).$$

Finally

$$\hat{\mathbf{n}}_2 \cdot \mathbf{q}_2 = q_2\ \hat{\mathbf{n}}_2 \cdot \left(\frac{\mathbf{q}_{\oplus 2}}{q_2} + \frac{\mathbf{P}_2}{q_2} \right) = q_2 \left(\hat{\mathbf{n}}_2 \cdot \hat{\mathbf{q}}_{\oplus 2} + \mathcal{O}\left(\frac{P_2}{q_2} \right) \right)$$

then

$$h_0 = 1 - \frac{q_{\oplus 2}^3\ \hat{\mathbf{n}}_2 \cdot \ddot{\mathbf{P}}_2}{\mu\ \hat{\mathbf{n}}_2 \cdot \mathbf{q}_2} + \mathcal{O}(\Delta t^2) + \mathcal{O}\left(\frac{P_2}{q_2} \right) = 1 - \Lambda_{n2} + \mathcal{O}(\Delta t^2) + \mathcal{O}\left(\frac{P_2}{q_2} \right)$$

where Λ_{n2} is the same quantity as Λ_n of eq. (28) computed at $t = t_2$.

The conclusion is that Gauss' method used with the heliocentric positions of the observer $\mathbf{q}_i = \mathbf{q}_{\oplus i} + \mathbf{P}_i$ is equivalent to the Topocentric Laplace's method of Section 3.2 to lowest order in Δt and neglecting the very small term $\mathcal{O}(P_2/q_2)$.

3.4 Problems in Topocentric Laplace's Method

Contrary to common belief, Laplace's method is not equivalent to Gauss': the latter is better, in that by using the observer position in eq. (19) and (20) it naturally accounts for topocentric observations. The question arises whether we could account for topocentric observations in Laplace's method (without iterations) by adding the term Λ_n from eq. (28). Surprisingly, the answer is already contained in the literature in a 100 year old paper by a famous author [Poincaré 1906, pag. 177–178]. To summarize the argument of Poincaré, plots showing the shape of the topocentric corrections as a function of time and a short citation are enough.

Figure 2

Figure 2 shows the simulated path of an approaching NEO as seen from an observing station (in this example in Hawaii). The darker portions of the curve indicate possible observations, the dotted ones are practically impossible, with an altitude $< 15°$. The apparent motion of the asteroid from night to night cannot be approximated using parabolic motion segments fitted to a single night[3]. For the geocentric path the parabolic approximation to $\hat{\boldsymbol{\rho}}(t)$, used by Laplace, would be applicable.

Figure 3

Figure 3 shows graphically that topocentric observations contain information beyond what is contained in the average angles and proper motion (the attributable, see Section 5). Thus, to reduce the observations to the

[3]Our translation of Poincaré: *It is necessary to avoid computing these quantities by starting from the law of rotation of the Earth.*

geocenter by removing the topocentric correction is not a good strategy.

Poincaré suggests computing what we call Λ_n by using a value of $\ddot{\mathbf{P}}$ obtained by interpolating the values $\mathbf{P}(t_i)$ at the times t_i of the observations (not limited to 3, one of the advantages of Laplace's method). This method could be used, but its practical advantages have not yet been established.

When the observations are performed from an artificial satellite (such as the Hubble Space Telescope or, in the future, from Gaia) the acceleration $\ddot{\mathbf{P}} \simeq 900\ cm\ s^{-2}$ and the Λ_n and Λ_v coefficients can be up to $\simeq 1,500$. A few hours of observations extending to several orbits can produce multiple kinks as in [Marchi et al. 2004, Figure 1] containing important orbital information.

4 Topocentric Qualitative Theory

In rectangular heliocentric coordinates (x, y) where the x axis is along $\hat{\mathbf{q}}_2$ (from the Sun to the observer) we have $\rho_2 = \sqrt{q_2^2 + x^2 + y^2 - 2xq_2}$ and $r_2 = \sqrt{x^2 + y^2}$, thus we can consider the function

$$C_0(x, y) = \frac{q_2}{\sqrt{q_2^2 + x^2 + y^2 - 2xq_2}} \left[h_0 - \frac{q_2^3}{(x^2 + y^2)^{3/2}} \right] .$$

The dynamical equation eq. (21) describes the level lines $C_0 = const$ in a bipolar coordinate system (r_2, ρ_2). Note that $C_0 = 0$ is the *zero circle* $r = r_0 = q/\sqrt[3]{h_0}$ for $h_0 > 0$ and is otherwise empty. The only stationary points of C_0 are the pairs (x, y) with $y = 0$ and x a solution of the equation $(h_0|x|^3 - q_2^3)x = 3q_2^3(x - q_2)$. For $h_0 \leq 0$ it has only one solution, x_1, with $0 < x_1 < q_2$. For $h_0 > 0$ there is always at least one solution $\bar{x} < -r_0 < 0$. If $0 < h_0 < 1$ there are two additional solutions, x_1 and x_2 such that $0 < x_1 <$

$q_2 < r_0 < x_2$. For $h_0 > 1$ there are no positive solutions[4].

Figure 4

The function $C_0(x, y)$ has a pole of order 3 at $(x, y) = (0, 0)$, with $\lim_{r_2 \to 0} C_0 = -\infty$, and a pole of order 1 at $(q_2, 0)$ with $\lim_{r_2 \to 0} C_0 = +\infty$ for $h_0 > 1$ and $= -\infty$ for $h_0 < 1$. If $h_0 = 1$, there is no unique limit value for $\rho_2 \to 0$, as shown by Figure 1.

4.1 Topology of the level curves of $C_0(x, y)$

The qualitative behavior of the level lines of $C_0(x, y)$ is different in the three cases $h_0 \leq 0$ (Figure 4), $0 < h_0 < 1$ (Figure 5) and $h_0 > 1$ (Figure 6).

The number of solutions of the dynamical equation (*i.e.* along a fixed topocentric direction) can be understood by evaluating the degree 8 polynomial (22) on the zero circle

$$P(r_0) = C_0^2 \, \frac{q^8}{h_0^{8/3}} \, \left(1 - h_0^{2/3}\right) \, .$$

Table 1

We summarize the possible numbers of solutions, for a given direction of observation ε, in the different cases, depending upon the value of h_0 and the sign of C, in Table 1. Note that in the Table we are not making the assumption of Charlier, that some solutions must exist, for the reasons given in Section 2.2. By spurious we mean a root of the polynomial (22) corresponding to $\rho \leq 0$ in eq. (21). This is not a complete qualitative theory replacing Charlier's for $h_0 = 1$, but already shows that the number of solutions can be

[4]The quantity C appearing in the topocentric Laplace's method defines exactly the same function of (x, y), with h_0 replaced by $1 - \Lambda_n$.

quite different from the classical case e.g., 2 solutions near opposition and up to 3 at low elongation. For a fully generalized qualitative theory, including the generalization of the *limiting curve*, see [Gronchi, 2007, in preparation].

Figure 5, Figure 6

4.2 Examples

Figure 7

We would like to find examples in which the additional solutions with respect to the classical theory by Charlier are essential. That is, cases in which the additional solutions provide a preliminary orbit closer to the true orbit, therefore leading to convergence of the least squares method, while the other preliminary solutions would fail to achieve this goal.

An example in which there are two solutions while observing in a direction close to the opposition is shown in Figure 7. The half line in the observing direction has two intersections with the relevant level curve of C_0. The nearer one, which has $\rho_2 = 0$ as counterpart in Charlier's theory, leads to a useful preliminary orbit. The farther one leads to a preliminary orbit with $e \simeq 10$. We have used the formulae of [Milani et al. 2004] to compute the maximum possible ρ_2 along the observation direction compatible with $e \leq 1$.

Another interesting feature is that the preliminary orbit using the nearer solution has residuals of the 6 observations with RMS = 66 arcsec while the one using the farther solution has RMS = 2.5 arcsec. This implies that if only one preliminary solution were passed to the next processing step by selecting the one with lowest RMS the good solution would be discarded. In this case,

to handle also the additional solution is essential not to lose the discovery.

Figure 8

To find an essential example with 3 solutions is not easy because in many cases the third solution, the nearest to the observer, has ρ_2 too small for the heliocentric 2-body approximation to be applicable. A value $\rho_2 \leq 0.01$ AU corresponds to the *sphere of influence* of the Earth, i.e., the region where the "perturbation" from the Earth is actually more important that the attraction from the Sun. Thus, a solution with such a small ρ_2 must be considered spurious, because the approximation used in Gauss' and Laplace's method is not valid.

To show how our arguments on the number of solutions applies to a real case (as opposed to the simulation of the example above) we have selected the asteroid 2002 AA_{29} and used observations from the first three nights (9, 11 and 12 January 2002). With the values $C_0 = 1.653$, $h_0 = 1.025$ we obtain from the observations and an elongation $\simeq 111^\circ$ there is only one solution with $\rho_2 = 0.045$ (see Figure 8, left), which easily leads to a full least squares solution with $\rho_2 = 0.044$. Although the value of h_0 is not very far from 1 the existence of the solution depends critically on $h_0 - 1 \neq 0$. If the value of h_0 had been set to 1 we would find no solution (see Figure 8, right).

4.3 Reliability and Precision

We need to implement the algorithms discussed in this paper for the computation of preliminary orbits in a way which is reliable enough for a large observation data set; we need to satisfy three requirements.

The first requirement is to obtain the solutions to the polynomial equations such as (22) in a way which is fast and reliable in providing the number of distinct real solutions. In this way we can fully exploit the understanding on the number of solutions (with topocentric observations) which we have achieved in this section. This is made possible by the algorithms computing the set of roots of a polynomial equation at once (as a complex vector) and with rigorous upper bounds for the errors, including roundoff. We use the algorithm by [Bini 1996] and the corresponding public domain software[5].

The second requirement is to improve the preliminary orbit as obtained from the solutions of the degree 8 polynomial equations in such a way that it is as close as possible to the least squares solution to be later obtained by differential corrections. There is such an immense literature on this topic that already [Merton 1925, page 693] started his paper with an ironic comment; in this paper it is not even appropriate to try and give complete references.

Conceptually, as shown by [Celletti and Pinzari 2005], each step in the iterative procedures used to improve the preliminary orbits (which they call *Gauss map*[6]) can be shown to increase the order in Δt of the approximation to the exact solutions of the 2-body equations of motion. However, [Celletti and Pinzari 2006] have also shown that iteration of a Gauss map can diverge when the solution of the degree 8 equation is far from the fixed point of the iterative procedure, outside of its convergence domain.

[5]For the Fortran 77 version `http://www.netlib.org/numeralgo/na10`. For Fortran 90 `http://users.bigpond.net.au/amiller/pzeros.f90` .

[6]The classical treatises, such as [Crawford et al. 1930], use the term *differential corrections* for algorithms of the same class of *Gauss map* in [Celletti and Pinzari 2005]. We follow the same terminology of the recent papers because, in modern usage, *differential corrections* refers to the iterative method to solve the least squares problem.

The same results apply to the algorithms, such as those of [Leuschner, 1913, Crawford et al. 1930], to improve the Laplace preliminary orbit. The difference between the two methods is that in Laplace's method the first approximation is with the observations treated as geocentric (or possibly corrected with an *assumed* distance, [Leuschner, 1913, page 15]), while in Gauss' method (Merton's version) the first approximation properly handles topocentric observations. This leads us to prefer Gauss' method.

We have implemented one of the available iterative improvement algorithms for Gauss' method and have found that it provides in most cases a preliminary orbit much closer to the least squares solution and therefore a more reliable first guess for the least squares algorithms. We have also found that the Gauss map diverges in a fraction of the test cases which is small, but still large enough to significantly decrease the efficiency of the algorithm (see Section 6.1). In some cases the number of orbits for which the Gauss map converges is less than the number of solutions of the degree 8 equations. It can happen that one of the lost degree 8 solutions was the only one leading to a least squares solution. One method to obtain the highest efficiency without an inordinate increase in the computational cost is to run two iterations, one with and one without the Gauss map. In the second iteration we also accept preliminary orbits with comparatively large residuals (up to a RMS of 100 arcsec), to allow for significant third body perturbations.

The third requirement is to use modified differential corrections algorithms with larger convergence domains in such a way that even when the geodetic curvature and the coefficients C and C_0 of the two methods are

poorly constrained by the available observations (because the arc length on the celestial sphere is too short) also a very rough preliminary orbit solution can lead to a least squares solution. This is discussed in the next section.

5 Weak preliminary orbits

An essential difference between the classical works on preliminary orbits and the modern approach to the same problem is that the effects of the astrometric errors cannot be neglected, especially in the operating condition of modern surveys: they try to use fewer observations, thus the deviations of the observed path from a great circle may not be significant.

5.1 Uncertainty of Curvature

The explicit computation of the two components of curvature of interest for orbit determination, geodesic curvature κ and along track acceleration $\dot{\eta}$, can be performed by using the properties of the orthonormal frame (1) by straightforward computation using the Riemannian structure of the unit sphere [Milani et al. 2007a, Section 6.4]. The results are

$$\kappa = \frac{1}{\eta^3} \left\{ (\ddot{\delta}\ \dot{\alpha} - \ddot{\alpha}\ \dot{\delta})\ \cos\delta + \dot{\alpha}\ \left[\eta^2 + (\dot{\delta})^2\right]\ \sin\delta \right\} = \kappa(\alpha, \delta, \dot{\alpha}, \dot{\delta}, \ddot{\alpha}, \ddot{\delta}) \quad (30)$$

$$\dot{\eta} = \frac{1}{\eta} \left[\ddot{\alpha}\ \dot{\alpha}\ \cos^2\delta + \ddot{\delta}\ \dot{\delta} - (\dot{\alpha})^2\ \dot{\delta}\ \cos\delta\ \sin\delta \right] = \dot{\eta}(\alpha, \delta, \dot{\alpha}, \dot{\delta}, \ddot{\alpha}, \ddot{\delta})\ . \quad (31)$$

Given these explicit formulae it is possible to compute the covariance matrix of the quantities $(\kappa, \dot{\eta})$ by propagation of the covariance matrix of the angles and their derivatives with the matrix of partial derivatives for κ and $\dot{\eta}$

$$\Gamma_{\kappa,\dot{\eta}} = \frac{\partial(\kappa, \dot{\eta})}{\partial(\alpha, \delta, \dot{\alpha}, \dot{\delta}, \ddot{\alpha}, \ddot{\delta})}\ \Gamma_{\alpha,\delta}\ \left[\frac{\partial(\kappa, \dot{\eta})}{\partial(\alpha, \delta, \dot{\alpha}, \dot{\delta}, \ddot{\alpha}, \ddot{\delta})}\right]^T\ . \quad (32)$$

The covariance matrix $\Gamma_{\alpha,\delta}$ for the angles and their first and second derivatives is obtained by the procedure of least squares fit of the individual observations to a quadratic function of time. The partials of κ and $\dot{\eta}$ are given below (note that the partials with respect to α are zero).

$$\begin{aligned}\frac{\partial\kappa}{\partial\delta} &= -\frac{1}{\eta^5}\Big[-2\,\dot\alpha^3\cos^2\delta\ \sin\delta\ \ddot\delta + \sin\delta\ \ddot\delta\,\dot\alpha\,\dot\delta^2 + 2\,\dot\alpha^2\cos^2\delta\ \sin\delta\ \ddot\alpha\,\dot\delta - \\ &- \sin\delta\ \ddot\alpha\,\dot\delta^3 - \dot\alpha^5\cos^3\delta\ - 4\,\dot\alpha^3\cos\delta\ \dot\delta^2 + \dot\alpha^3\cos^3\delta\ \dot\delta^2 - 2\,\dot\alpha\ \cos\delta\ \dot\delta^4\Big]\end{aligned}$$

$$\frac{\partial\dot\eta}{\partial\delta} = -\frac{\dot\alpha}{2\ \eta^3}\Big[\sin(2\delta)\ \Big(\dot\alpha^2\ \ddot\alpha\ \cos^2\delta + 2\ \dot\delta^2\ \ddot\alpha - \dot\alpha\ \dot\delta\ \ddot\delta\Big) + 2\,\dot\alpha\ \dot\delta^3\ \cos(2\delta) + 2\,\dot\alpha^3\dot\delta\ \cos^4\delta\Big]$$

$$\frac{\partial\kappa}{\partial\dot\alpha} = \frac{1}{\eta^5}\Big[-\dot\alpha\ \cos^3\delta\ \Big(2\,\dot\alpha\ \ddot\delta - 3\,\dot\delta\ \ddot\alpha\Big) + \dot\delta^2\ \Big(\ddot\delta\ \cos\delta - \dot\alpha^2\cos^2\delta\ \sin\delta + 2\,\dot\delta^2\ \sin\delta\Big)\Big]$$

$$\frac{\partial\dot\eta}{\partial\dot\alpha} = -\frac{\cos\delta\ \ \dot\delta}{\eta^3}\ \Big[-\cos\delta\ \ \ddot\alpha\,\dot\delta + \dot\alpha^3\sin\delta\ \cos^2\delta\ + 2\,\dot\alpha\ \sin\delta\ \dot\delta^2 + \cos\delta\ \ddot\delta\,\dot\alpha\Big]$$

$$\frac{\partial\kappa}{\partial\dot\delta} = -\frac{1}{\eta^5}\Big[\cos\delta\ \Big(\dot\alpha^2\ \ddot\alpha\ \cos^2\delta - 2\,\dot\delta^2\ \ddot\alpha + 3\,\dot\alpha\ \dot\delta\ \ddot\delta\Big) - \dot\alpha\ \dot\delta\ \sin\delta\ \Big(\dot\alpha^2\ \cos^2\delta - 2\,\dot\delta^2\Big)\Big]$$

$$\frac{\partial\dot\eta}{\partial\dot\delta} = -\frac{\dot\alpha\ \cos^2\delta}{\eta^3}\ \Big[-\ddot\delta\,\dot\alpha + \dot\alpha^3\cos\delta\ \sin\delta\ + \ddot\alpha\,\dot\delta\Big]$$

$$\frac{\partial\kappa}{\partial\ddot\alpha} = -\frac{\dot\delta\ \cos\delta}{\eta^3}\quad,\quad \frac{\partial\kappa}{\partial\ddot\delta} = \frac{\dot\alpha\ \cos\delta}{\eta^3}\quad,\quad \frac{\partial\dot\eta}{\partial\ddot\alpha} = \frac{\dot\alpha\ \cos^2\delta}{\eta}\quad,\quad \frac{\partial\dot\eta}{\partial\ddot\delta} = \frac{\dot\delta}{\eta}\ .$$

The last four of these partials, the 2×2 matrix $\partial(\kappa,\dot\eta)/\partial(\ddot\alpha,\ddot\delta)$, contribute to the principal part of the covariance of $(\kappa,\dot\eta)$ for short arcs, see below.

We use a full computation of the covariance matrix without approximations to assess the significance of curvature by using the formula from [Milani et al. 2007a]

$$\chi^2 = \begin{bmatrix}\kappa\\ \dot\eta\end{bmatrix}^T\ \Gamma^{-1}_{\kappa,\dot\eta}\ \begin{bmatrix}\kappa\\ \dot\eta\end{bmatrix} \tag{33}$$

and we assume that the curvature is *significant* if $\chi^2 > \chi^2_{min} = 9$.

5.2 The Infinite Distance Limit

The problem of low values of C can occur in two ways: near the zero circle and for large values of both ρ and r. On the other hand, the uncertainty in the estimates of the deviations from a great circle will depend upon the length of the observed arc (both in time Δt and in arc length $\sim \eta\,\Delta t$). For short observed arcs it may be the case that the curvature is not significant. Then the preliminary orbit algorithms will yield orbits which may fail as starting guesses for differential corrections.

We will now focus on the case of distant objects. We would like to estimate the order of magnitude of the uncertainty in the computed orbit with respect to the small parameters ν, τ, b where ν is the astrometric accuracy of the individual observations (in radians) and $\tau = n_\oplus \Delta t$, $b = q_\oplus/\rho$ are small for short observed arcs and for distant objects, respectively. Note that the proper motion η for $b \to 0$ has principal part $n_\oplus\, b$ – the effect of the motion of the Earth. The uncertainty in the angles (α, δ) and their derivatives can be estimated as follows (see [Crawford et al. 1930, page 68])

$$\Gamma_{\alpha,\delta} = \mathcal{O}(\nu) \quad , \quad \Gamma_{\dot\alpha,\dot\delta} = \mathcal{O}(\nu\tau^{-1}) \quad , \quad \Gamma_{\ddot\alpha,\ddot\delta} = \mathcal{O}(\nu\tau^{-2})\ .$$

The uncertainty of the curvature components $(\kappa, \dot\eta)$ should be estimated by the propagation formula (32) but it can be shown that the uncertainty of $(\delta, \dot\alpha, \dot\delta)$ contributes with lower order terms. Thus we use the estimates

$$\frac{\partial(\kappa,\dot\eta)}{\partial(\ddot\alpha,\ddot\delta)} = \begin{bmatrix} \mathcal{O}(b^{-2})\ n_\oplus^{-2} & \mathcal{O}(b^{-2})\ n_\oplus^{-2} \\ \mathcal{O}(1) & \mathcal{O}(1) \end{bmatrix}$$

and obtain

$$\Gamma_{\kappa,\dot\eta} = \nu \begin{bmatrix} \mathcal{O}(b^{-4}\tau^{-2}) & \mathcal{O}(b^{-2}\tau^{-2}) n_\oplus^2 \\ \mathcal{O}(b^{-2}\tau^{-2}) n_\oplus^2 & \mathcal{O}(\tau^{-2}) n_\oplus^4 \end{bmatrix}\ .$$

To propagate the covariance to the variables $(\rho, \dot{\rho})$ we use the implicit equation connecting C and ρ, obtained by eliminating r from (7) and (21)

$$F(C,\rho) = C\ \frac{\rho}{q_\oplus}\ + \frac{q_\oplus^3}{(q_\oplus^2+\rho^2+2q_\oplus\rho\cos\varepsilon)^{3/2}}\ - 1 + \Lambda_n = 0\ . \tag{34}$$

For $b \to 0$ we have $C\ b^{-1} \to 1$; thus $C \to 0$ and is of the same order as the small parameter b. Although C depends upon all the variables $(\alpha, \delta, \dot{\alpha}, \dot{\delta}, \ddot{\alpha}, \ddot{\delta})$, its uncertainty mostly depends upon the uncertainty of κ and thus, ultimately, upon the difficulty in estimating the second derivatives of the angles. Next, we compute the dependence of $\Gamma_{\rho,\dot{\rho}}$ upon $\Gamma_{\kappa,\dot{\eta}}$. From the derivatives of the implicit function $\rho(\kappa)$, assuming $\cos\varepsilon, \eta, \hat{\mathbf{n}}$ to be constant and keeping only the term of lowest order in q/ρ,

$$\frac{\partial\rho}{\partial\kappa} = -\frac{\eta^2\ q^4}{\mu\ \hat{\mathbf{q}_\oplus}\cdot\hat{\mathbf{n}}}\ \frac{\rho}{q_\oplus\ C} + \mathcal{O}\left(\frac{q^3}{\rho^3}\right) = q_\oplus\ \mathcal{O}(1)\ .$$

In the same way from (29) we deduce $\dot{\eta} = n_\oplus^2\ \mathcal{O}(b)$ and the estimates

$$\frac{\partial\dot{\rho}}{\partial\kappa} = n_\oplus\ q_\oplus\ \mathcal{O}(1) \quad , \quad \frac{\partial\dot{\rho}}{\partial\dot{\eta}} = \frac{q_\oplus}{n_\oplus}\ \mathcal{O}(b^{-2})\ .$$

For the covariance matrix

$$\Gamma_{\rho,\dot{\rho}} = \frac{\partial(\rho,\dot{\rho})}{\partial(\kappa,\dot{\eta})}\ \Gamma_{\kappa,\dot{\eta}}\ \left[\frac{\partial(\rho,\dot{\rho})}{\partial(\kappa,\dot{\eta})}\right]^T$$

we compute the main terms of highest order in b^{-1}, τ^{-1} as

$$\Gamma_{\rho,\dot{\rho}} = \nu\ b^{-3}\ \tau^{-2}\ \begin{bmatrix} q_\oplus^2\ \mathcal{O}(1) & q_\oplus^2\ n_\oplus\ \mathcal{O}(1) \\ q_\oplus^2\ n_\oplus\ \mathcal{O}(1) & q_\oplus^2\ n_\oplus^2\ \mathcal{O}(1) \end{bmatrix}\ . \tag{35}$$

In conclusion, if $(\rho, \dot{\rho})$ are measured in the appropriate units (AU for ρ and $n_\oplus$ AU for $\dot{\rho}$) their uncertainties are of the same order and none of the two will be better determined than the other.

This conclusion appears different from [Bernstein and Khushalani 2000], who claim that for a TNO observed arc with low curvature the inverse distance $1/\rho$ can be determined in a robust way, while the other variable $\dot{\rho}/\rho$ remains essentially undetermined. In fact, by propagating the covariance from eq. (35) to the variables $(1/\rho, \dot{\rho}/\rho)$ and expressing them in the natural units $1/q_\oplus, n_\oplus$ we find that the RMS of $\dot{\rho}/\rho$ is larger by a factor $1/b$ than the one of $1/\rho$. Thus there is no disagreement; however, the purpose of whatever preliminary orbit is to use them as first guess for differential corrections.

The coordinates $(\rho, \dot{\rho})$, together with $(\alpha, \delta, \dot{\alpha}, \dot{\delta})$, form a set of *Attributable Orbital Elements* with the special property that the confidence region of solutions with low residuals is a very thin neighborhood of a portion of the $(\rho, \dot{\rho})$ plane [Milani et al. 2005b, Section 3]; a similar property, with a different plane, is shared by the Cartesian Elements. Thus these coordinates are very suitable for differential corrections, performed under conditions of quasi-linearity even for large corrections; a set of coordinates containing $(1/\rho, \dot{\rho}/\rho)$ results in a much larger nonlinearity, with increased risk of divergence.

We do agree with [Bernstein and Khushalani 2000] that for a TNO observed only over an arc shorter than one month there is very often an approximate degeneracy forcing the use of a constrained orbit (with only 5 free parameters). The *weak direction*, along which an arbitrary choice needs to be made, is in the $(\rho, \dot{\rho})$ plane, may vary and is generally not close to the $\dot{\rho}$ axis [Milani et al. 2005b, Figures 3-6]. In the context of the tests on TNOs orbits described in Section 6.1, for simulated discoveries around opposition we found that the weak direction forms an angle with the ρ axis (computed with

the scaling indicated by eq. (35)) between $-31°$ and $+17°$. Near quadrature it forms an angle with the $\dot{\rho}$ axis between $-54°$ and $+36°$. The weak direction depends upon the elongation; actually [Bernstein and Khushalani 2000] warn that their arguments are not applicable exactly at opposition.

5.3 From Preliminary to Least Square Orbits

The procedure to compute an orbit given an observed arc with ≥ 3 nights of data (believed to belong to the same object) begins with the solution of the degree 8 equation (22) and ends with the differential corrections iterations to achieve a full least squares orbit, with 6 solved parameters. For algorithms more efficient than the classical ones there are up to four intermediate steps:

1. an iterative *Gauss map* to improve the solution of the degree 8 equation;
2. adding to the preliminary orbit(s) another one, obtained from the *Attributable* and a value for $(\rho, \dot{\rho})$ selected inside the *Admissible Region* (see details below);
3. a fit of the available observations to a 4-parameter attributable; the values of ρ and $\dot{\rho}$ are kept fixed at the previous values;
4. a fit of the available observations constrained to the *Line Of Variations (LOV)*, a smooth line defined by minimization on hyperplanes orthogonal to the weak direction of the normal matrix.

Intermediate step 1 has been discussed in Section 4.3.

By *Attributable* we mean the set of 4 variables $(\alpha, \delta, \dot{\alpha}, \dot{\delta})$ estimated at some reference time by a fit to the observations [Milani et al. 2001]. It is

possible to complete an attributable to a set of orbital elements by adding the values of range and range rate $(\rho, \dot{\rho})$ at the same time. For each attributable we can determine an *Admissible Region* which is a compact set in the $(\rho, \dot{\rho})$ plane compatible with Solar System orbits [Milani et al. 2004].

For intermediate step 2 we need to distinguish two cases depending upon the topology of the Admissible Region [Milani et al. 2004]. If it has two connected components (this occurs for distant objects observed near opposition) we select the point which is the center of symmetry of the component far from the observer. This corresponds to an orbit with $0 \leq e < 1$; note that, sometimes, a circular orbit may be incompatible with the Attributable.

If the Admissible Region is connected then we select the point along the symmetry line $\dot{\rho} = const$ at 0.8 times the maximum distance ρ compatible with $e \leq 1$. This case always occurs near quadrature; if the object is indeed distant, thus has a low proper motion η, the selected point is also far.

In any case, the selected point $(\rho, \dot{\rho})$ in the Admissible Region completed with the Attributable provides an orbit compatible with the given Attributable and belonging to the Solar System; this is called a *Virtual Asteroid (VA)* [Milani 2005]. This VA method provides an additional preliminary orbit. This does not matter when there are already good preliminary orbits computed with Gauss' method; we shall see in Section 6.1 that for TNOs this additional preliminary orbit is often required, in most cases near quadrature, because the curvature is hardly significant.

Intermediate Step 3 is essentially the method proposed by D. Tholen, available in his public domain software KNOBS. It has already been tested in

the context of a simulation of a next generation survey in [Milani et al. 2006].

Intermediate Step 4 is fully described in [Milani et al. 2005a]. Our preferred options are to use either Cartesian or Attributable Elements scaled as described in [Milani et al. 2005a, Table 1], that is, consistently with eq. (35).

The steps listed above are all optional and indeed it is possible to compute good orbits in many cases without some of them. However, if the goal is a very reliable algorithm, a smart connecting logic is necessary. As an example, Step 1 is used in a first iteration, omitted in a second one. Step 2 is essential for distant objects. Step 3 is used whenever the curvature is not significant, i.e., when the observed arc is of type 1 [Milani et al. 2007a], which can be tested by eq. (33). Step 4 is important for weakly determined orbits, otherwise the differential corrections may diverge when starting from an initial guess with comparatively large residuals. Even then, Step 4 may fail and, in turn, diverge under differential corrections. In this case the differential corrections restart from the outcome of the previous step. This connecting logic is an extension of the one presented in [Milani et al. 2005a, Figure 5].

6 Tests

The tests use a *Solar System Model* – a catalog of orbits of synthetic objects [Milani et al. 2006]. Given assumed observation scheduling and instrument performance we compute the *detections* of the catalog objects above a threshold signal to noise ratio. We then add astrometric error to these observations, with the presumed accuracy of the future surveys (about 0.1 arcsec). We have not included false detections (corresponding to no synthetic object).

Then we assemble into *tracklets* the detections, from the same observing night, which could belong to the same object. The tracklets are assembled in *tracks* from several distinct nights; in this context, at least three nights are required. For these simulations we have used the algorithms of [Kubica et al. 2007] to assemble both tracklets and tracks.

When the number density of detections per unit area is low both tracklets and tracks are (almost always) *true*, i.e., they contain only detections of one and the same synthetic object. When the number density is large, as expected from the next generation surveys, both tracklets and tracks can be *false*, i.e., containing detections belonging to different objects. This is why a track needs to be confirmed by computing an orbit: first a preliminary orbit, then by differential corrections another orbit which fits all the observations in the least squares sense. The structure containing the track and the derived orbit with the accessory data for quality control (covariance, weights and residuals, statistical tests) is called an *identification* [Milani et al. 2007b].

The purpose of the tests is to measure the performance of the algorithms described in this paper, according to the following criteria:

- Efficiency E: the fraction of true tracks for which good preliminary and least squares orbits were calculated.

- Accuracy A: the fraction of returned orbits that correspond to true tracks. I.e., the orbit computation should fail on false tracks (either no preliminary orbit or no least squares orbit or residuals too large).

- Goodness G: the fraction of least squares orbits close enough to the

ground truth orbits to allow later recovery (e.g., in another lunation).

A speed criterion (based on CPU time) is less important, because computing power grows as fast as the astrometric data rate[7]. Still, we need to check that the very large data sets expected in the near future can be processed with reasonable computational resources.

These are not performance tests for surveys like Pan-STARRS or LSST. The purpose is to show that, whatever the rate of new objects discoveries, they will not be lost because of inefficiency in the orbit determination.

6.1 Small targeted tests

Since the orbits of MBAs and Jupiter Trojans are easier to compute than NEOs and more distant objects [Milani et al. 2006], to assess the Efficiency of these algorithms we have prepared four targeted simulations: two containing only observations of NEOs and two with TNOs only. In both cases, one simulation surveys near opposition and the other the so called *sweet spots*, at solar elongations between 60° and 90°. The most relevant metrics is Efficiency: Accuracy is not an issue because the number density per is small (indeed, Accuracy is 100% in all tests of this Subsection).

Table 2

The first part of Table 2 refers to the simulation for NEOs around opposition. Incomplete Identifications occur because the simulation included two lunations and the algorithm used to assemble the tracks cannot handle an

[7]By Moore's law the number of elements on a chip grows exponentially with time: this affects the number of pixels in a CCD and the speed of computers. The CCD array is the main cause of the data increase from Pan-STARRS and LSST, but not the only one.

observed arc of more than a month (which would have an excessive curvature [Kubica et al. 2007, Section 8.2]). The separate orbits obtained in the two lunations for the same object can be joined later with other algorithms, see [Milani et al. 2001]. Thus there is a negligible number of true tracks which have not been confirmed by the orbit computation.

The lower part of Table 2 refers to the simulation including only NEOs at the sweet spots. In the NEO simulations the Efficiency is very high but could be improved, especially at the sweet spots, with increased computational intensity; however, this could impair Accuracy for larger data sets.

All of the cases left without an orbit, although a true track was proposed, resulted from a failure of the preliminary orbit, in most cases because the degree 8 equation has only spurious roots (in the sense of Section 4.2). The VA method was not of any help, as expected since it is intended for low curvature cases. In other cases some useful preliminary orbit was discarded because the RMS of the fit was large, between 200 and 300 arcsec.

Table 3

The upper part of Table 3 refers to the simulation with TNOs around opposition. The Incomplete Identifications for 6-nighters occur for the same reasons of the NEO case. The lower part of Table 3 refers to the simulation for TNOs in the sweet spot regions. Overall, there are only 3 cases of failed orbit determination, and these are due to very tight quality control thresholds.

Table 4

The preliminary orbit algorithms have not shown even one case of failure in the TNO simulations. We need to assess the proportion of this success due

to the Virtual Asteroid method, expected to be especially effective for the low curvatures typical of TNOs. We have rerun the simulation without the VA method: at opposition, and even more in the sweet spots, giving up the VA method would result in a significant loss of TNO discoveries (Table 4, column "No VA"). The conclusion is that the VA method is essential for TNOs while it is almost irrelevant for NEOs.

Did the effort in reliably handling double (even triple) preliminary orbit solutions significantly improve the performance in the NEO case? We have rerun with only one preliminary orbit, the one with lowest RMS of residuals, passed to differential corrections. The results (Table 4, column "1 Pre") clearly show that for NEOs near quadrature to pass to differential corrections multiple preliminary orbits is essential for top Efficiency.

Another test has been to stop after the first of the two iterations (see Section 5.3), the one with a tighter control in the RMS of the residuals for the 2-body preliminary orbit (set at 10 arcsec in these tests) and using the Gauss map. The results (column "1st It.") are that the second iteration has no effect on TNOs but is relevant for NEOs especially in the sweet spots.

We need to assess how much the improved differential corrections (discussed in Section 5.3) have contributed to the success of these simulations.

For column "No 4fit" the 4-parameter fit step was not used. The results, essentially identical to the "No VA" case, indicate that the two algorithms must be used together for TNOs. Column "No LOV" indicates that the step with the 5-parameter least squares fit to obtain a LOV solution has a very large effect for TNOs. We get the worst results (column "LSQ") if neither

the 4-fit algorithm nor the LOV solutions are used and the preliminary orbits are passed directly to a full 6-parameters differential corrections.

The column labeled "Best" refers to the best combination of innovative and improved algorithms found so far; by comparing with the other columns the differences are important, thus all the steps discussed in Sections 4 and 5 are essential to achieve the best results for both NEOs and TNOs.

6.2 Large scale tests

The main purpose of a large scale test is to measure the Accuracy. Efficency can be affected by Accuracy: when there are *Discordant Identifications* (with some tracklets in common) and they cannot be merged in one with all the tracklets of both, there is no way to choose which of the two is true. Then we have to discard both, which means losing true identifications and decreasing Efficiency. By keeping both we would decrease Accuracy, with each false identification introducing permanent damage to the quality of the results[8].

We have prepared simulations for one lunation of a next generation survey both near opposition and the sweet spots. The assumed limiting magnitude was V=24 and the Solar System model was used at full density, including the overwhelming majority of MBAs (11 million synthetic objects, 10 M MBAs, 269 K NEOs, 28K TNOs); Table 5 gives the size of the dataset. The focus of this paper is on the objects for which tracklets are available in three nights. Objects observed for less nights are part of the problem in that their tracklets can be incorrectly identified: for such large number densities false

[8] *False facts are highly injurious to the progress of science, for they often endure long...*, C. Darwin, *The Origin of Man*, 1871.

identifications easily happen [Milani et al. 2006, figure 3].

Table 5

The first Accuracy problem occurs at the tracklet composition stage: some tracklets are false, i.e., mix detections belonging to different objects. The question is whether they are identified.

The second Accuracy problem occurs at the track composition stage. A track is just a *hypothesis of identification* to be checked by computing an orbit: at a high tracklet number density most of the tracks are false. The *Overhead* is the ratio between the total number of proposed tracks and true ones: it was large, at the sweet spots even above what was found in previous simulations [Kubica et al. 2007, Table 3].

The question is whether the orbit determination stage can produce the true orbits with good Efficiency and still reject almost all the false tracks. To achieve this, the residuals of the best fit orbits need to be submitted to a rigorous statistical quality control. Our residuals quality control algorithm uses the following 10 metrics (control values in square brackets)

- RMS of astrometric residuals divided by the assumed RMS of the observation errors (=0.1 arcsec in these simulations) [1.0]
- RMS of photometric residuals in magnitudes [0.5]
- bias of the residuals in RA and in DEC [1.5]
- first derivative of the residuals in RA and in DEC [1.5]
- second derivative of the residuals in RA and in DEC [1.5]

- third derivative of the residuals in RA and in DEC [1.5]

To compute the bias and derivatives of the residuals we fit them to a polynomial of degree 3 and divide the coefficients by their standard deviation as obtained from the covariance matrix of the fit[9].

Table 6

The results are summarized in Tables 6 and 7. As expected, the main problem is in Accuracy. Notwithstanding the tight statistical quality controls on residuals, while processing tens of millions of proposed tracks a few thousands false tracks are found to fit well all their observations (columns "False"). The numbers are small with respect to the total number of tracks but they are not negligible as a fraction of the true tracks (columns "%"). A much smaller number of false tracks contains some false tracklets (columns "F.Tr."): even the presence of a significant fraction of false tracklets affects neither Efficiency nor Accuracy.

The false identifications result from combining tracklets from 2 (or 3) distinct simulated objects. With a fit passing all the quality controls, we cannot a priori discard any of them: only by consulting the ground truth can we know they are false. By further tightening the quality control parameters we may remove many false but some true identifications as well. The values of the controls used are already the result of adjustment suggested by experiments to find a good trade off between Accuracy and Efficiency.

The most effective method to remove false tracks is obtained by not con-

[9]When these algorithms are used on real data additional metrics should assess the outcome of outlier removal [Carpino et al., 2003]. For simulations this does not apply.

sidering each identification by itself but globally. We have previously defined the *normalization* of lists of identifications in [Milani et al. 2005b, Section 7] and [Milani et al. 2006, Section 6]. It removes duplications and inferior identifications but also rejects all the Discordant Identifications. This is not because they are all presumed false, indeed very often one true and one false identification are Discordant, but we do not know which is which, unless one of the two has a significantly better fit. If the difference in the normalized RMS of the astrometric residuals is more than 0.25 we keep the best; otherwise we remove both and sacrifice Efficiency for Accuracy.

Table 7

The results of the normalization procedure are shown on the right hand side of Table 6: the false tracks can be reduced to a negligible number in this way, but the Efficiency also changes as a result of the normalization. In Table 7 the rows indicate how the results differ according to the orbital class of the simulated objects. The row "Com" includes Centaurs, long and short period comets. The sweet spots simulation does not include Jupiter Trojans because the Trojan swarms were not near quadrature. The columns "Eff.%" show the Efficiency before, "Eff.No.%" after normalization.

Are the results of Tables 6 and 7 satisfactory and, if not, what else can be done? The Efficiency for NEOs and TNOs is not affected by normalization (because of the lower number densities). Maybe losing a few percent of MBAs is not important. Nevertheless, even this problem can be solved together with the other, possibly more important, of the few NEOs and comets lost.

By separately analyzing the Efficiency of the three steps of the procedure

(track composition, orbit computation, normalization) we found that the algorithm to generate tracks has been 97.6% and 98.7% efficient at opposition and at the sweet spots, respectively. The orbit computation procedure on the proposed true tracks has been 99.8% and 99.3% efficient. The normalization procedure has been 98.6% and 99.4% efficient. The performances of the three steps are well balanced and there is some room for improvement, but not much[10]. The solution is to use a two iteration procedure.

The normalization procedure generates two outputs: the new list of identifications and the list of *leftover* tracklets which have not been *used* in the confirmed identifications: thus the set of tracklets is sharply reduced, simplifying further processing. When two tracklets have detections in common, if one of the two is included in a confirmed identification then the other can be also be considered used: Table 8 shows that the normalization is effective in discarding false tracklets, thus confirming with a full scale simulation what had been found with the small simulation of [Milani et al. 2006].

Table 8

The leftover tracklets can be used as input to another iteration with different controls. Because of the reduced number density of tracklets, Accuracy should be less of a problem. We can also use for a second iteration an independent algorithm, e.g., the one already proposed and tested on large simulations [Milani et al. 2005b] and on small real data sets [Boattini et al. 2007].

A full discussion of the iteration strategies for the next generation surveys

[10]Moderately loosening the controls for track composition could improve the overall Efficiency, which is the product of the Efficiency of the three steps. An excessive loosening would increase the rate of false identification, thus the loss at the normalization stage.

is beyond the scope of this paper. However, to show that the normalized Efficiency values of Table 7 are not a problem, we have run an improved version of the recursive attribution algorithms of [Milani et al. 2005b] on the leftover tracklets. To control the false identifications we have used even tighter quality controls. The results are in Table 9, showing an almost complete recovery of the orbits lost for whatever reason in the previous processing.

Table 9

The same procedure allows also to compute normalized identifications for 2-nighters, with Efficiency and Accuracy as described in Table 10. After this, the leftover tracklets mostly contain 1-nighters.

Table 10

The best way to assess Goodness is to mimic as much as possible how the results from one lunation would be used in the next one. We have made two opposition simulations for consecutive lunations. Given the 3-nighter identifications for the first month we try to attribute to them some tracklets in the other month. This procedure has been 99.6%, 99.7% and 99.9% efficient for objects with 1, 2 and 3 tracklet in the second lunation, respectively. There were no NEOs among the few cases of failed/incomplete attribution.

7 Conclusions and Future Work

The purpose of this paper was to identify efficient algorithms to compute preliminary and least squares orbits given a track (or proposed identification).

We have found suitable algorithms by revising the classical *preliminary orbit* methods. The most important improvements are provisions to keep

alternate solutions under control. The existence of double solutions was known since long time and we have shown that even triple solutions can occur. Still there is no reason this should impair the orbit determination performance, provided these cases are handled with due care.

For the *differential corrections* stage, leading from preliminary orbits to least squares ones, we have adopted innovative algorithms already available from previous work (by ourselves and others). If properly combined by a control logic they significantly improve the efficiency of differential corrections even when the preliminary orbits are not close to the nominal solutions.

The third stage of orbit determination is the *quality control* of the results, based upon statistical analysis of the residuals. With a small number of objects this may appear unnecessary. With the high detection density expected soon this will be critical, because tracklets belonging to different objects may be incorrectly identified. To remove false identifications is not easy: we have found the method of *normalization* to be very effective for this purpose, but unavoidably some true identifications are sacrificed to remove the discordant false ones. We need to select options and details of the algorithms such that the number of false is kept low but few true ones are lost.

Although our mathematically rigorous theoretical results do not need confirmation it has been useful to test their practical performance on simulations of the next generation surveys. In this way we have shown that orbits can be computed even for the most difficult classes of orbits. We have also shown, with full density simulations including an overwhelming majority of MBAs, that the large number of objects observed does not result in a "false

identification catastrophe". On the contrary, a large number density is compatible with a low number of lost objects provided the quality control on the residuals is tight enough and the sequence of algorithms is suitably chosen.

The performance for identification and orbit determination critically depends upon the individual algorithms and upon the *pipeline design* - the sequence of algorithms operating one upon the output of another. We have used the algorithms from [Kubica et al. 2007] as the first step, followed by the ones of this paper as the second step. We have mentioned the possibility of using the algorithms of [Milani et al. 2005b] as the third step. Even more complicated pipelines can be conceived, but the discussion of pipeline design is beyond the scope of this paper and will be the subject of future work.

Another future work is the definition of the procedure to combine the results from different lunations of a large survey. We have done a test with a second lunation by using the *attribution* algorithm of [Milani et al. 2001]. In case a survey has been operating for years, other algorithms such as the ones of [Milani et al. 2000] and [Kubica et al. 2007] may become necessary.

In the three papers [Milani et al. 2005b], [Kubica et al. 2007] and the present one we have defined a number of algorithms to be used to process astrometric data of Solar System objects when the number density will be much larger than they are now. This will very soon be the case with Pan-STARRS and LSST. Such algorithm definition work is a necessary step to exploit their superior survey performance and provide orbits for most observed objects. In the near future we will handle real data which will contain unpredicted problems and present a new, formidable challenge.

Acknowledgments

Milani & Gronchi are supported by the Italian Space Agency through contract 2007-XXXX, Knežević from Ministry of Science of Serbia through project 146004 "Dynamics of Celestial Bodies, Systems and Populations". Jedicke & Denneau by the Panoramic Survey Telescope and Rapid Response System at the University of Hawaii's Institute for Astronomy, funded by the United States Air Force Research Laboratory (AFRL, Albuquerque, NM) through grant number F29601-02-1-0268. Pierfederici by the LSST project funded by the National Science Foundation under SPO No. 9 (AST-0551161) through Cooperative Agreement AST-0132798, by private donations and in-kind support at DoE laboratories and other LSSTC Members.

References

[Bernstein and Khushalani 2000] Bernstein, G., Khushalani, B., 2000. Orbit Fitting and uncertainties for Kuiper belt objects. AJ 120, 3323-3332.

[Bini 1996] Bini, D.A., 1996. Numerical Computation of Polynomial Zeros by Means of Aberth's Method. Numerical Algorithms 13, 179-200.

[Boattini et al. 2007] Boattini, A., Milani, A., Gronchi, G. F., Spahr, T., Valsecchi, G. B., 2007. Low solar elongation searches for NEOs: a deep sky test and its implications for survey strategies. In Milani, A. et al. (Eds.), Near Earth Objects, our Celestial Neighbors: Opportunity and Risk. Cambridge University Press, pp. 291-300.

[Carpino et al., 2003] Carpino, M., Milani, A., Chesley, S. R., 2003. Error Statistics of Asteroid Optical Astrometric Observations. Icarus 166, 248-270.

[Celletti and Pinzari 2005] Celletti, A. and Pinzari, G., 2005. Four Classical Methods for Determining Planetary Elliptic Elements: A Comparison. CMDA 93, 1-52.

[Celletti and Pinzari 2006] Celletti, A. and Pinzari, G., 2006. Dependence on the observational time intervals and domain of convergence of orbital determination methods. CMDA 95, 327-344.

[Charlier 1910] Charlier, C. V. L., 1910. On Multiple Solutions in the Determination of Orbits from three Observations. MNRAS 71, 120-124.

[Charlier 1911] Charlier, C. V. L., 1911. Second Note on Multiple Solutions in the Determination of Orbits from three Observations. MNRAS 71, 454-459.

[Crawford et al. 1930] Crawford, R. T., Leuschner, A. O., Merton, G., 1930. Determination of orbits of comets and asteroids. McGraw Hill, New York.

[Danby 1962] Danby, J. M. A., 1962. Fundamentals of Celestial Mechanics. The Macmillan Company, New York.

[Gauss 1809] Gauss, C. F., 1809. Theory of the Motion of the Heavenly Bodies Moving about the Sun in Conic Sections. Reprinted by Dover, 1963.

[Herrick 1971] Herrick, S., 1971. Astrodynamics, Volume 1. van Nostrand Reinhold Co., London.

[Ivezić et al. 2007] Ivezić, Ž., Tyson, J. A., Jurić, M., Kubica, J., Connolly, A., Pierfederici, F., Harris, A. W., Bowell, E., and the LSST Collaboration, 2007. LSST: Comprehensive NEO Detection, Characterization, and Orbits. In Milani, A. et al. (Eds.), Near Earth Objects, our Celestial Neighbors: Opportunity and Risk. Cambridge University Press, pp. 353–362.

[Jedicke et al. 2007] Jedicke, R., Magnier, E. A., Kaiser, N., Chambers, K. C., 2007. The next decade of Solar System discovery with Pan-STARRS. In Milani, A. at el. (Eds.), Near Earth Objects, our Celestial Neighbors: Opportunity and Risk. Cambridge University Press, pp.341–352.

[Kubica et al. 2007] Kubica, J., Denneau, L., Grav, T., Heasley, J., Jedicke, R., Masiero, J., Milani, A., Moore, A., Tholen, D., Wainscoat, R. J., 2007. Efficient intra- and inter-night linking of asteroid detections using kd-trees. Icarus 189, 151–168.

[Laplace 1780] Laplace, P. S., 1780. Mém. Acad. R. Sci. Paris. In *Laplace's collected works* 10, pp. 93–146.

[Leuschner, 1913] Leuschner, A. O., 1913. A short method of determining orbits from 3 observations. Publ. Lick Obs. 7, 3–20.

[Leuschner, 1913] Leuschner, A. O., 1913. Short methods of determining orbits, second paper. Publ. Lick Obs. 7, 217–376.

[Marchi et al. 2004] Marchi, S., Momany, Y., Bedin, L. R., 2004. Trails of solar system minor bodies on WFC/ACS images. New Astronomy 9, 679–685.

[Marsden 1985] Marsden, B. G., 1985. Initial orbit determination: the pragmatist's point of view. Astron. J. 90, 1541–1547.

[Merton 1925] Merton, G., 1925. A modification of Gauss's method for the determination of orbits. MNRAS 85, 693–732.

[Milani 2005] Milani, A., 2005. Virtual asteroids and virtual impactors. In Knežević, Z., Milani, A. (Eds.) Dynamics of Populations of Planetary Systems. Cambridge University Press, pp. 219–228.

[Milani et al. 2000] Milani, A., La Spina, A., Sansaturio, M. E., Chesley, S. R., 2000. The Asteroid Identification Problem III. Proposing identifications. Icarus 144, 39–53.

[Milani et al. 2001] Milani, A., Sansaturio, M. E., Chesley, S. R., 2001. The Asteroid Identification Problem IV: Attributions. Icarus 151, 150–159.

[Milani et al. 2004] Milani, A., Gronchi, G. F., de' Michieli Vitturi, M., Knežević, Z., 2004. Orbit Determination with Very Short Arcs. I Admissible Regions. CMDA 90, 59–87.

[Milani et al. 2005a] Milani, A., Sansaturio, M. E., Tommei, G., Arratia, O., Chesley, S. R., 2005a. Multiple solutions for asteroid orbits: computational procedure and applications. Astron. Astrophys. 431, 729–746.

[Milani et al. 2005b] Milani, A., Gronchi, G. F., Knežević, Z., Sansaturio, M. E., Arratia, O., 2005b. Orbit Determination with Very Short Arcs. II Identifications. Icarus 79, 350–374.

[Milani et al. 2006] Milani A., Gronchi, G. F., Knežević, Z., Sansaturio, M. E., Arratia, O., Denneau, L., Grav, T., Heasley, J., Jedicke, R., Kubica, J., 2006a. Unbiased orbit determination for the next generation asteroid/comet surveys. In D. Lazzaro et al. (Eds.) Asteroids Comets and Meteors. Cambridge University Press, pp. 367–380.

[Milani et al. 2007a] Milani, A., Gronchi, G. F., Knežević, Z., 2007. New Definition of Discovery for Solar System Objects. EMP 100, 83–116.

[Milani et al. 2007b] Milani, A., Denneau, L., Pierfederici, F., Jedicke, R., 2007. Data Exchange Standard for solar system object detections and orbits, version 2.02. Pan-STARRS project, Honolulu, PSDC-530-004-01.

[Plummer 1918] Plummer, H. C., 1918. An introductory treatise on Dynamical Astronomy. Cambridge University press, reprinted by Dover, New York., 1960.

[Poincaré 1906] Poincaré, H., 1906. Sur la détermination des orbites par la méthode de Laplace. Bulletin astronomique 23, 161–187.

[Virtanen 2003] Virtanen, J., Tancredi, G., Muinonen, K., Bowell, E., 2003. Orbit computation for transneptunian objects. Icarus 161, 419–430.

Table 1: The number of preliminary orbit solutions. Prelim: the number of preliminary orbit solutions (for a given C and h_0). Roots: the number of positive roots of the polynomial equation (22). Spurious: the number of spurious roots.

		Prelim.	Roots	Spurious
$h_0 \leq 0$	$\mathcal{C} < 0$	1 or 3	1 or 3	0
	$\mathcal{C} > 0$	0	1 or 3	1 or 3
$0 < h_0 < 1$	$\mathcal{C} < 0$	1 or 3	1 or 3	0 or 2
	$\mathcal{C} > 0$	0 or 2	1 or 3	1 or 3
$h_0 = 1$	$\mathcal{C} < 0$	0 or 1 or 2	1 or 3	1 or 2 or 3
	$\mathcal{C} > 0$	0 or 1 or 2	1 or 3	1 or 2 or 3
$h_0 > 1$	$\mathcal{C} < 0$	0 or 2	1 or 3	1 or 3
	$\mathcal{C} > 0$	1 or 3	1 or 3	0 or 2

Table 2: For each of the NEO simulations, separately for objects observed on a different number of nights, the columns give: [1] Total number of objects, [2] Number of Complete Identifications (containing all the tracklets belonging to the object), [3] Efficiency (defined as [2]/[1], in %), [4] Number of incomplete Identifications, [5] Fraction [4]/[1] in % of incomplete Identifications, [6] Number of objects lost (no confirmed Identification), [7] Fraction [6]/[1] in % lost.

	[1]	[2]	[3]	[4]	[5]	[6]	[7]
Observed					Inc.		Lost
Arc	Total	Compl.	Effic.	Inc.	Fraction	Lost	Fraction
Opposition							
3-nighters	1123	1119	99.6%	0	0.0%	4	0.4%
6-nighters	123	0	0.0%	123	100.0%	0	0.0%
Sweet Spots							
3-nighters	397	389	98.0%	0	0.0%	8	2.0%
6-nighters	63	0	0.0%	63	100.0%	0	0.0%

Table 3: For each of the TNO simulations the same data as in Table 2.

Observed Arc	[1] Total	[2] Compl.	[3] Effic.	[4] Inc.	[5] Inc. Fraction	[6] Lost	[7] Lost Fraction
Opposition							
3-nighters	2005	2001	99.8%	3	0.15%	1	0.05%
6-nighters	670	0	0.0%	670	100.0%	0	0.00%
Sweet Spots							
3-nighters	2493	2491	99.9%	0	0.00%	2	0.08%

Table 4: Fraction of lost 3-nighters using different algorithms. The methods used for each column are detailed in the text.

Simulation	Best	1 Pre	1st It.	No VA	No 4fit	No LOV	LSQ
NEO Opp.	0.40%	0.50%	3.2%	0.4%	0.4%	0.4%	0.4%
NEO Sw.	2.00%	13.4%	18.1%	2.3%	2.3%	2.8%	2.8%
TNO Opp.	0.05%	0.05%	0.05%	38.3%	38.4%	45.7%	47.7%
TNO Sw.	0.10%	0.10%	0.10%	75.3%	75.3%	82.6%	82.8%

Table 5: Simulated data sets: [1] survey region, [2] number of tracklets, [3] of which false, [4] number of simulated objects with observed tracklets, [5] of which with tracklets in 3 different nights, [6] overhead (see text), [7] objects with tracklets in 2 different nights, [8] with tracklets in only 1 night.

[1] Region	[2] Tracklets	[3] False	[4] Objects	[5] 3-night	[6] Overhead	[7] 2-night	[8] 1-night
Oppos.	654315	26006	253289	164333	222.8	41244	47712
Sweet sp.	695067	59253	283831	144903	501.3	62177	76751

Table 6: Accuracy Results: before and after normalization, total number of false identifications accepted, percentage (with respect to the total number of identifications), number of identifications containing false tracklets.

Region	All Identifications			Normalized		
	False	%	F.Tr.	False	%	F.Tr.
Oppos.	7093	4.31	4	80	0.05	1
Sweet sp.	1869	1.30	10	29	0.02	0

Table 7: Efficiency Results: total number of objects, Efficiency, Efficiency after Normalization, at opposition and at sweet spots, overall and for each orbital class.

Obj.Type	Opposition			Sweet Spots		
	Total	Eff.%	Eff.No.%	Total	Eff.%	Eff.No.%
All	161146	97.3	95.9	144903	98.0	97.4
MBA	154700	97.3	95.8	135911	98.0	97.4
NEO	353	90.4	90.4	271	80.1	80.1
Tro				6894	97.9	97.8
Com	665	98.6	97.6	253	98.0	97.6
TNO	5428	97.7	97.7	1574	98.7	98.7

Table 8: Leftover tracklets: number of tracklets not included in confirmed identifications, and the fractional reduction of the tracklets dataset; the same data for False tracklets.

Survey region	Leftover tracklets	Reduction %	Leftover False	Reduction %
Opposition	168122	74.3%	5363	79.4%
Sweet spots	232101	66.6%	17033	71.2%

Table 9: Identifications recovered with recursive atttribution: fraction of the objects lost in the first iteration which have been recovered, combined Efficiency from both iterations, fraction of false identifications; total and for NEOs only.

	Recovered Objects	Efficiency	False Identifications
Opposition	75.4%	99.0%	0.06%
NEOs	85.3%	97.1%	0
Sweet Spots	75.0%	99.4%	0.02%
NEOs	85.2%	97.1%	0

Table 10: 2-night identifications, normalized.

Survey region	Efficiency	False Identifications
Opposition	83.4%	2.1%
Sweet spots	89.2%	1.3%

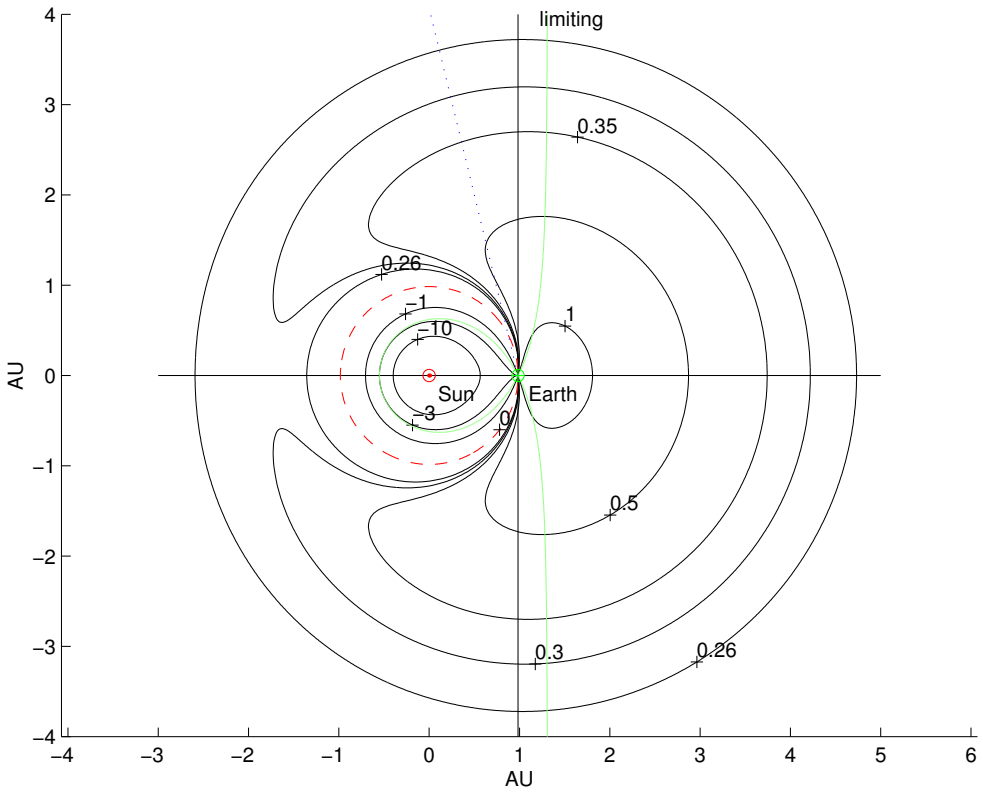

Figure 1: Level curves of $C(r, \rho)$ (solid lines), limiting curve (labeled), zero circle (dashed). For a given value of C and an observation direction (dotted) there can be either 1 or 2 solutions, e.g., for $C = 0.3$ there are 2.

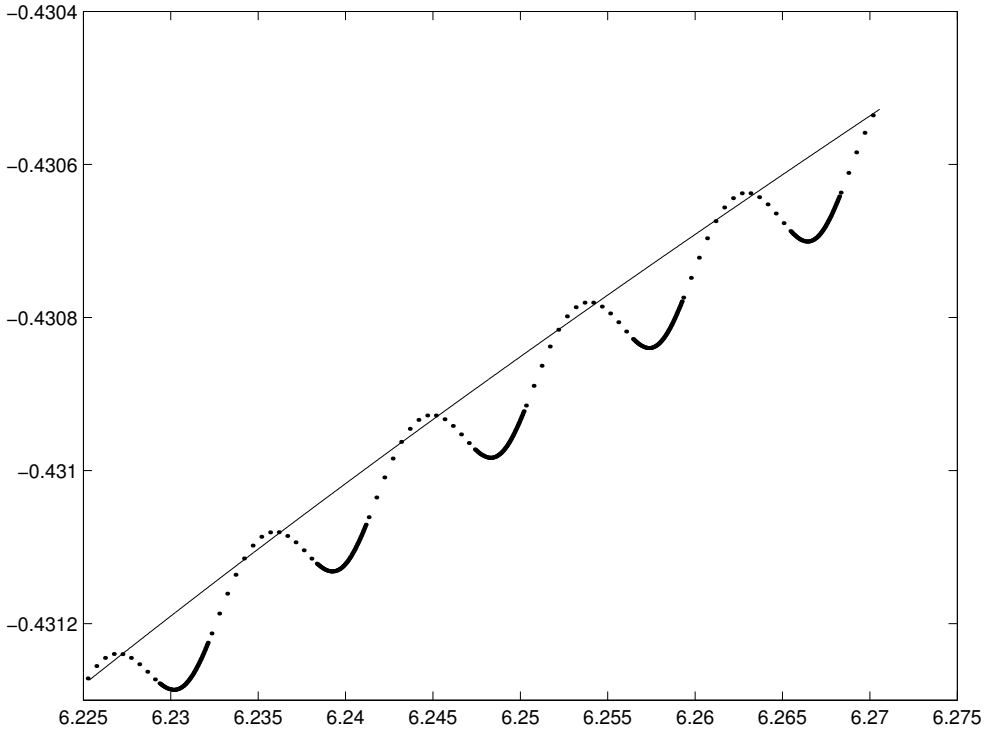

Figure 2: The path in the sky of an approaching NEO. This example is (101955) 1999 RQ_{36} as it would have been seen in July 2005 if an observatory on Mauna Kea had been observing continously. The solid portions of the curve indicate possible observations, the dotted ones are practically impossible, with an altitude $< 15°$. The continuous curve gives simulated observations from the geocenter. Cordinates are RA and DEC in radians.

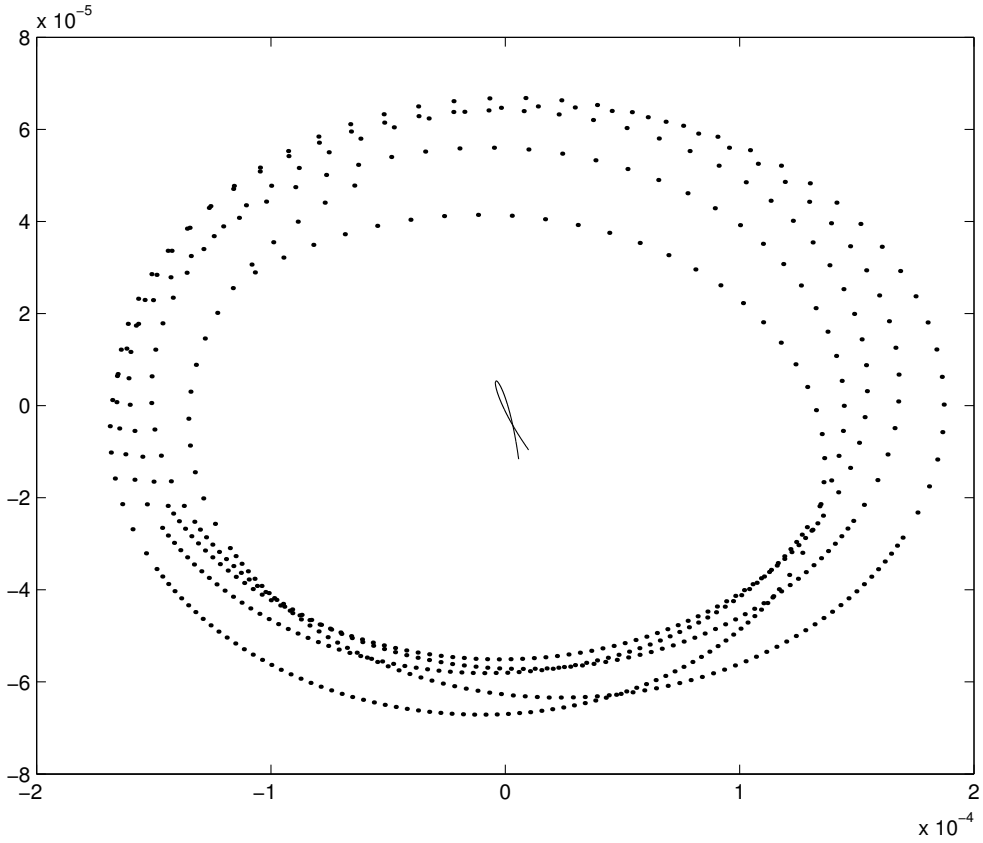

Figure 3: The same data as in the previous figure after removing the best fitting linear functions of time in both coordinates. In this case the curves represent the content of information beyond the attributable. The larger loop is from Mauna Kea, with the densest portion corresponding to possible observations; the small curl near $(0, 0)$ is for a geocentric observer. Coordinates are differences in RA and DEC in radians.

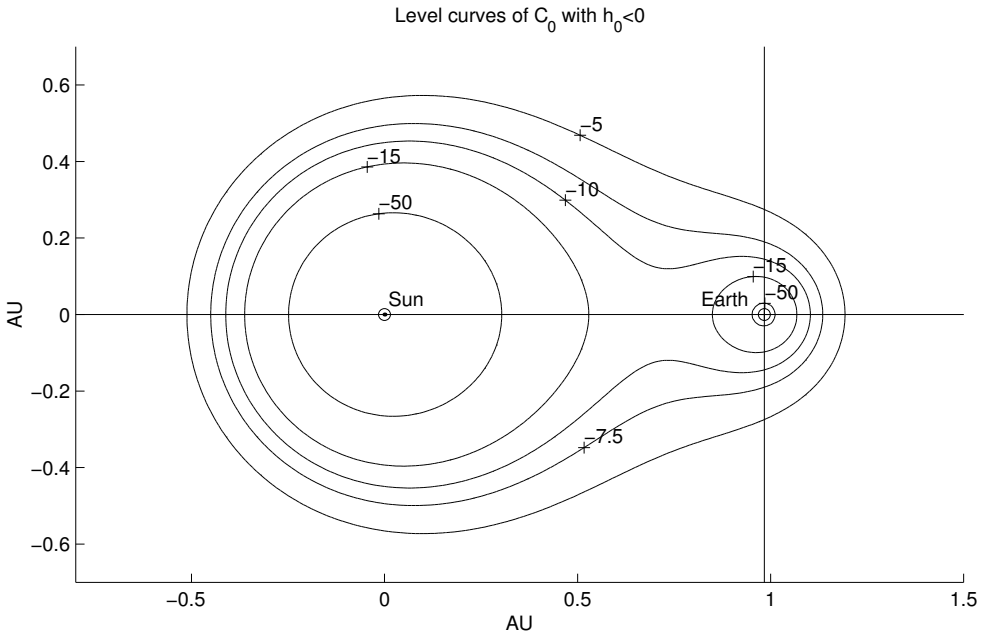

Figure 4: Level curves of $C_0(x, y)$ for $h_0 = -0.5$. Note there is no zero circle.

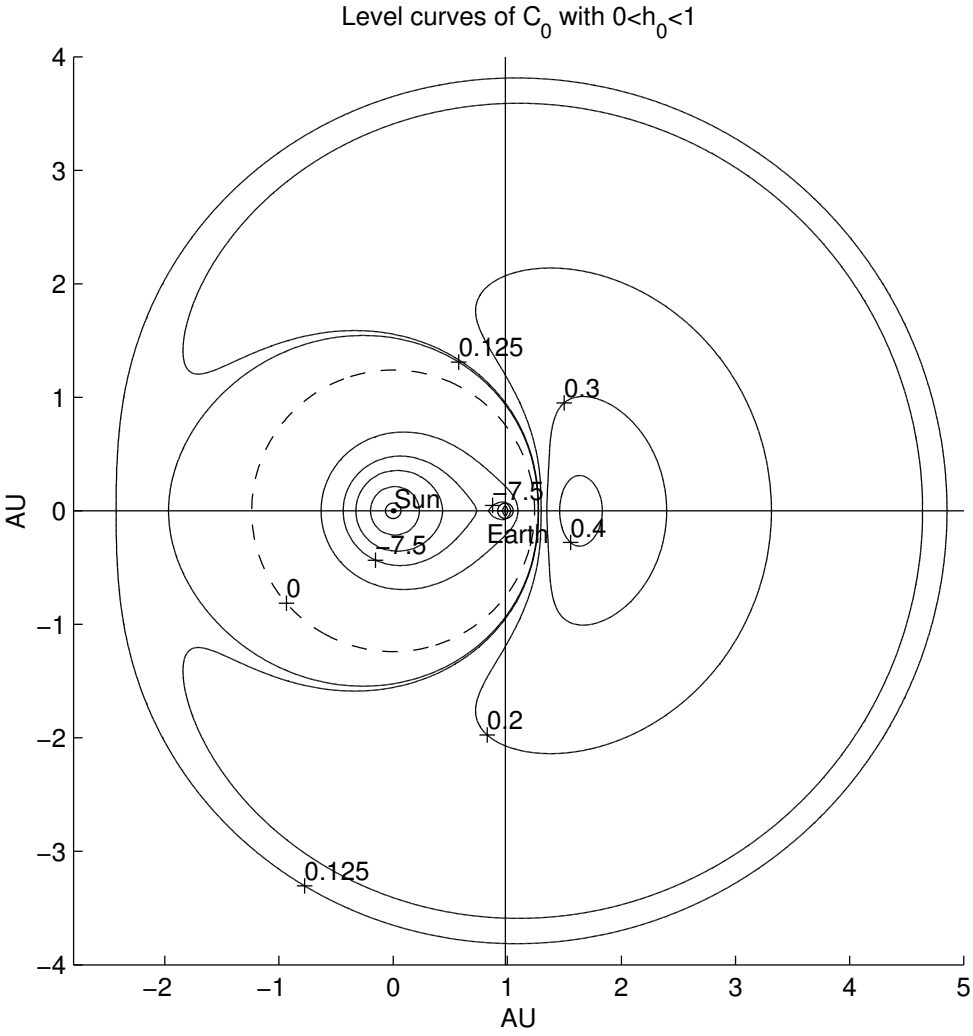

Figure 5: Level curves of $C_0(x, y)$ for $h_0 = 0.5$, including the zero circle (dashed).

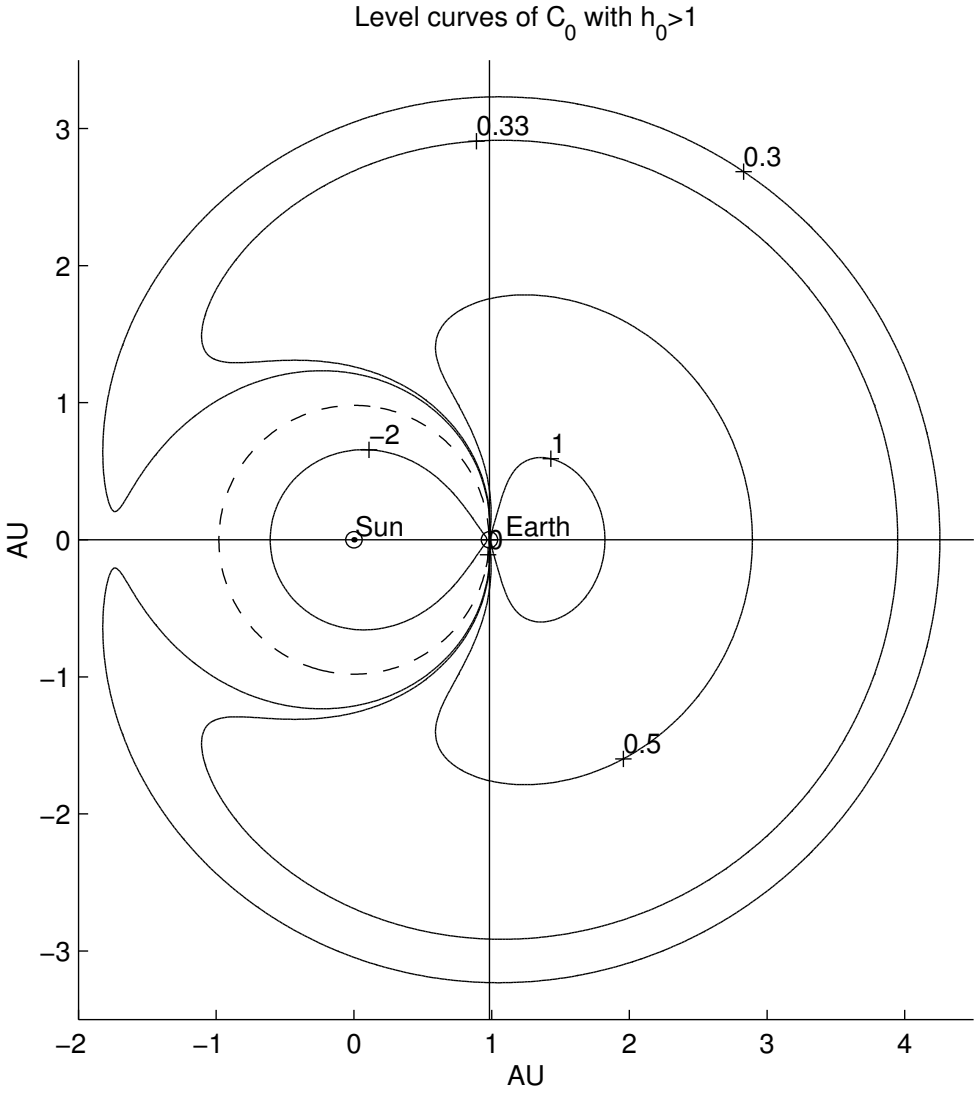

Figure 6: Level curves of $C_0(x, y)$ for $h_0 = 1.01$, including the zero circle (dashed).

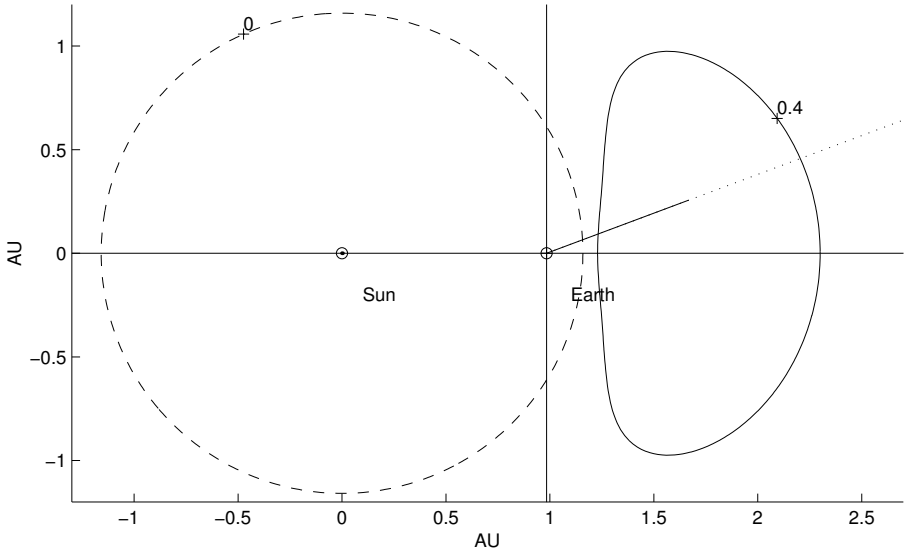

Figure 7: An example with two solutions near opposition: for $h_0 = 0.613$ the direction of observation (dotted) has two intersections with the level curve $C_0(x, y) = 0.4$ (continuous); the zero circle is dashed. The positions in the observation direction with a bounded orbit are drawn as a continuous line.

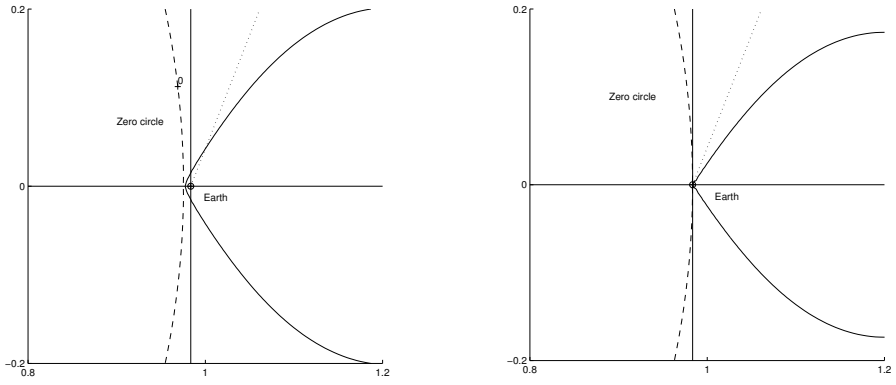

Figure 8: For the preliminary orbit of 2002 AA_{29} the relevant level curve ($C_0 = 1.653$) is shown (continuous) in the same plane of Figure 1; the zero circle (dashed) and the observation direction (dotted) are also shown. Left: using the actual value $h_0 = 1.025$. Right: using a value of $h_0 = 1$ that does not account for the topocentric correction. Units are AU for both axes.